Journal of
Medicinal Chemistry

Article

Structure–Activity Relationships in 1,4-Benzodioxan-Related Compounds. 8. {2-[2-(4-Chlorobenzyloxy)phenoxy]ethyl}-[2-(2,6-dimethoxyphenoxy)ethyl]amine (Clopenphendioxan) as a Tool to Highlight the Involvement of □- and □-Adrenoreceptor Subtypes in the Regulation of Human PC-3 Prostate Cancer Cell Apoptosis and Proliferation

Wilma Quaglia, Giorgio Santoni, Maria Pigini, Alessandro Piergentili, Francesco Gentili, Michela Buccioni, Michela Mosca, Roberta Lucciarini, Consuelo Amantini, Massimo Ivan Nabissi, Patrizia Ballarini, Elena Poggesi, Amedeo Leonardi, and Mario Giannella

J. Med. Chem., **2005**, 48 (24), 7750-7763• DOI: 10.1021/jm0580398 • Publication Date (Web): 02 November 2005

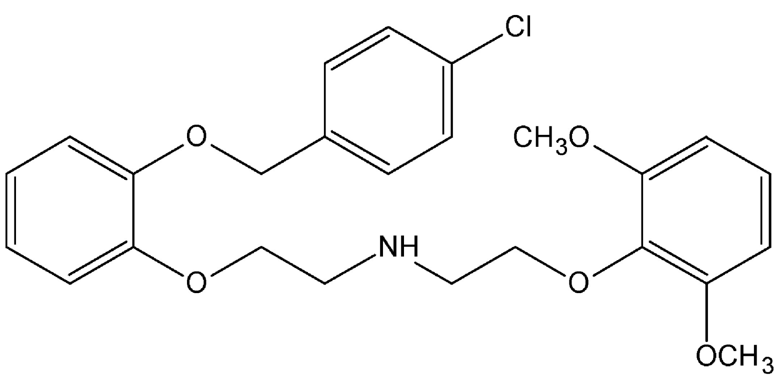

7, Clopenphendioxan

Structure−Activity Relationships in 1,4-Benzodioxan-Related Compounds. 8.[1] {2-[2-(4-Chlorobenzyloxy)phenoxy]ethyl}-[2-(2,6-dimethoxyphenoxy)ethyl]amine (Clopenphendioxan) as a Tool to Highlight the Involvement of α_{1D}- and α_{1B}-Adrenoreceptor Subtypes in the Regulation of Human PC-3 Prostate Cancer Cell Apoptosis and Proliferation

Wilma Quaglia,[§] Giorgio Santoni,[‡] Maria Pigini,[§] Alessandro Piergentili,[§] Francesco Gentili,[§] Michela Buccioni,[§] Michela Mosca,[‡] Roberta Lucciarini,[‡] Consuelo Amantini,[‡] Massimo Ivan Nabissi,[‡] Patrizia Ballarini,[||] Elena Poggesi,[⊥] Amedeo Leonardi,[⊥] and Mario Giannella*[,§]

Dipartimento di Scienze Chimiche, Università degli Studi di Camerino, via S. Agostino 1, 62032 Camerino, Italy, Dipartimento di Medicina Sperimentale e Sanità Pubblica, Università degli Studi di Camerino, via Scalzino, 62032 Camerino, Italy, Dipartimento di Biologia Molecolare, Cellulare e Animale, Università degli Studi di Camerino, via Camerini, 62032 Camerino, Italy, and Divisione Ricerca e Sviluppo Farmaceutici, Recordati S. p. A., via Civitali 1, 20148 Milano, Italy

Received August 3, 2005

A series of new α_1-adrenoreceptor antagonists (**5**−**18**) was prepared by introducing various substituents (Topliss approach) into the ortho, meta, and para positions of the benzyloxy function of the phendioxan open analogue **4** ("openphendioxan"). All the compounds synthesized were potent antagonists and generally displayed, similarly to **4**, the highest affinity values at α_{1D}- with respect to α_{1A}- and α_{1B}-AR subtypes and 5-HT_{1A} subtype. By sulforhodamine B (SRB) assay on human PC-3 prostate cancer cells, the new compounds showed antitumor activity (estimated on the basis of three parameters GI_{50}, TGI, LC_{50}), at low micromolar concentration, with **7** ("clopenphendioxan") exhibiting the highest efficacy. Moreover, this study highlighted for the first time α_{1D}- and α_{1B}-AR expression in PC3 cells and also demonstrated the involvement of these subtypes in the modulation of apoptosis and cell proliferation. A significant reduction of α_{1D}- and α_{1B}-AR expression in PC3 cells was associated with the apoptosis induced by **7**. This depletion was completely reversed by norepinephrine.

Introduction

The α_1-adrenoreceptors (α_1-ARs) belong to the superfamily of G-protein-coupled receptors and, on the basis of pharmacological and binding studies, have been subdivided into at least three subtypes, namely α_{1A} (α_{1a}), α_{1B} (α_{1b}), and α_{1D} (α_{1d}), with upper and lower case subscripts being used to designate the native or recombinant receptor, respectively.[2] An additional α_1-AR subtype (α_{1L}), characterized by low affinity for prazosin, seems to be a functional phenotype of the α_{1A} subtype.[3]

At the peripheral level, α_1-ARs are expressed in a wide variety of tissues, including liver, kidney, blood vessels, heart, and prostate. The α_{1A}-, α_{1B}-, and α_{1D}-AR subtypes are differentially localized in human prostate, with α_{1A}-AR believed to be predominant in the fibromuscular stroma, but not in the glandular epithelium,[4] while α_{1B}-AR is mainly localized in the epithelium[5] and α_{1D}-AR principally detected in the stroma and blood vessels.[6]

Few studies have been reported on the expression of α_1-AR subtypes on prostate cancer cells. α_{1A}-AR expression, both at mRNA and protein levels, has been detected in the human androgen-dependent lymph node carcinoma of the prostate (LNCap) cancer cells,[7] while no detectable α_{1A}-AR mRNA expression has been found in the androgen-independent human prostate PC-3 and DU-145 cancer cells.[8] No data concerning the expression of α_{1B}- and α_{1D}-AR in prostate cancer cells have been so far provided.

Some α_1-AR antagonists are already in use for clinical treatment of benign prostatic hyperplasia (BPH).[9] Their therapeutic effects may be attributed to not only reduced prostatic smooth muscle tone but also inhibition of nonepithelial (stromal and smooth muscle cells) cell proliferation.

Recent studies have demonstrated that α_1-AR antagonists, such as doxazosin and terazosin, induce apoptosis in primary human prostate cancer epithelial cells, DU-145 and PC-3, and smooth muscle cells, without affecting cell proliferation.[8] The mechanisms of apoptosis induction seem to be α_{1A}-AR independent.[8,10] Putative mechanisms underlying doxazosin-mediated apoptosis include the up-regulation of transforming growth factor beta (TGF-beta) signaling effectors[11,12] and blocking of intracellular protein kinase B/Akt activation.[13] Terazosin-induced PC-3 and DU-145 cancer cells death is p53- and Rb-independent and is associated with G1 phase cell cycle arrest, up-regulation of p27Kip1 and Bax, and down-regulation of bcl-2,[14−16] and I kappa B alpha induction.[12]

The role of α_1-ARs in agonist-stimulated proliferation has mainly been demonstrated for smooth muscle myocytes, although there is evidence that these receptors may participate in the promotion of other cell types

* To whom correspondence should be addressed. Phone: +39 0737 402257. Fax +39 0737 637345. E-mail: mario.giannella@unicam.it.
[§] Dipartimento di Scienze Chimiche, Università degli Studi di Camerino.
[‡] Dipartimento di Medicina Sperimentale e Sanità Pubblica, Università degli Studi di Camerino.
[||] Dipartimento di Biologia Molecolare, Cellulare e Animale, Università degli Studi di Camerino.
[⊥] Recordati S.p.A.

10.1021/jm0580398 CCC: $30.25
Published on Web 11/02/2005

Chart 1

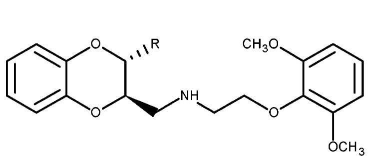

1 (WB 4101), R = H
2 (phendioxan), R = C_6H_5
3 (mephendioxan) R = p-CH_3-C_6H_4

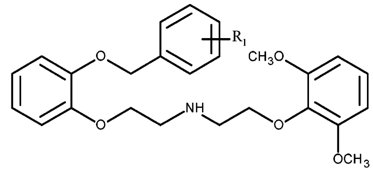

4, R_1 = H	**11**, R_1 = o-NO_2
5, R_1 = o-Cl	**12**, R_1 = m-NO_2
6, R_1 = m-Cl	**13**, R_1 = p-NO_2
7, R_1 = p-Cl	**14**, R_1 = o-OCH_3
8, R_1 = o-CH_3	**15**, R_1 = m-OCH_3
9, R_1 = m-CH_3	**16**, R_1 = p-OCH_3
10, R_1 = p-CH_3	**17**, R_1 = p-OC_2H_5
	18, R_1 = p-$OCH(CH_3)_2$

including prostate cells.[17−19] In this respect, growing evidence supports the role of α_1-ARs in the direct mitogenic effect of catecholamines on prostate growth.[20]

α_1-Adrenergic stimulation of human prostate stromal and vascular smooth muscle increases DNA synthesis and cell proliferation via p44/42 (ERK1/2) MAPK activation.[21,22] The identity of the α_1-AR subtypes involved in the norepinephrine (NE)-mediated stimulating effects in prostatic nonepithelial cells are still unknown, whereas the involvement of α_{1D}-AR subtype has been suggested.[22] Finally, in human LNCap androgen-dependent prostate cancer cells, epinephrine-induced prostate cancer cell proliferation was inhibited by the competitive α_1-AR antagonists, prazosin and WB4101.[7]

In continued efforts to identify potent and selective α_1-AR antagonists, we previously reported the discovery of compounds prepared by subsequent modifications of WB 4101 (**1**):[23] the insertion of a phenyl ring or a p-tolyl moiety at the 3-position having a trans relationship with the 2-side chain led to phendioxan (**2**)[24] and mephendioxan (**3**),[25] the latter proving significantly selective for α_{1A}-AR subtype relative to both α_{1B} and α_{1D} subtypes. Subsequently, the opening of the benzodioxan ring of **2** afforded *N*-[2-[2-benzyloxyphenoxy]ethyl]-*N*-[2-(2,6-dimethoxyphenoxy)ethyl]amine (**4**), showing high potency and significant selectivity for α_{1D} subtype with respect to the α_{1A} and α_{1B} subtypes.[26] The name of "openphendioxan" has now been given to compound **4**. In the present study, in an attempt to further improve the α_{1D}-AR selectivity of **4**, while obviously maintaining its high affinity, various substituents were introduced into the ortho, meta, and para positions of the aromatic ring of the benzyloxy function (compounds **5**−**18**) (Chart 1), with the aim to recognize possible ancillary binding sites. In fact, it is known that the aromatic areas play a critical role in the interaction of α_1-AR antagonists with the corresponding receptors.[27,28] The substituents were chosen using the Topliss approach, which takes into account the electronic, lipophilic, and steric factors for substitution on a phenyl ring, using basic Hansch principles in a noncomputerized manner.[29,30]

Compounds **5**−**18** were evaluated for their affinity for the α_1-AR subtypes and their prostate antitumor activity with respect to unsubstituted lead **4**, and doxazosin was used as a reference.[31] Furthermore, an in-depth investigation was conducted to determine the α_1-AR subtypes expression in the human PC-3 prostate cancer cell line used in this study. Finally, the ability of compound **7** and the lead **4** to inhibit the α_1-AR-dependent growth of PC-3 cells by inducing apoptosis and/or inhibiting cell proliferation was evaluated.

Scheme 1[a]

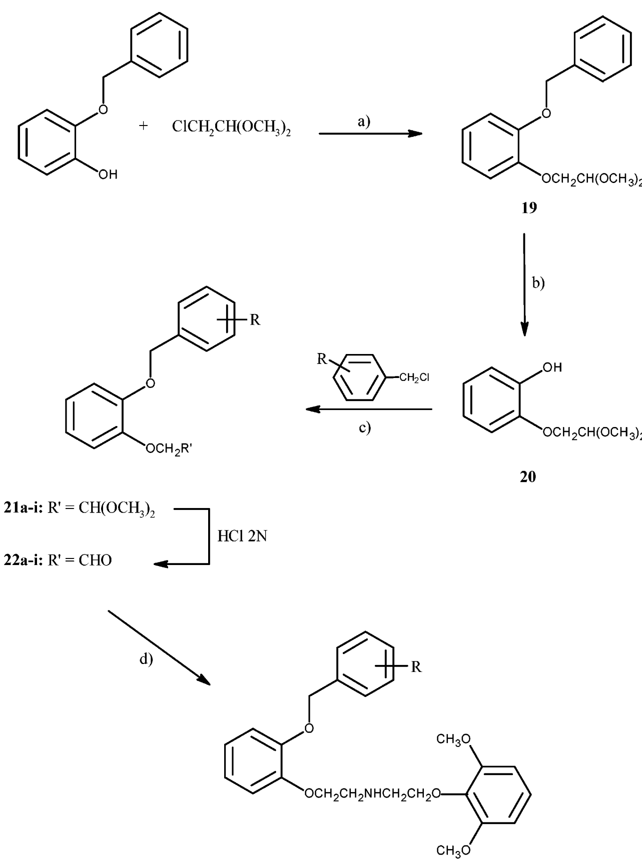

5 - 7: R = o, m, p-Cl
8-10: R = o, m, p-CH_3
11-13: R = o, m, p-NO_2

[a] Reagents: (a) NaH/DMF; (b) H_2/Pd; (c) K_2CO_3/DMF; (d) 2-(2,6-dimethoxyphenoxy)ethylamine,[32] $NaBH_3CN$/EtOH.

Chemistry. The new compounds **5**−**18** were synthesized according to the methods reported in Schemes 1−3. Alkylation of 2-(benzyloxy)phenol with 2-chloro-1,1-dimethoxyethane gave 1-(2,2-dimethoxyethoxy)-2-[(benzyl)oxy]benzene (**19**). 2-(2,2-Dimethoxyethoxy)-phenol (**20**) obtained by catalytic hydrogenation of **19** was then alkylated with the appropriate benzyl chlo-

Scheme 2[a]

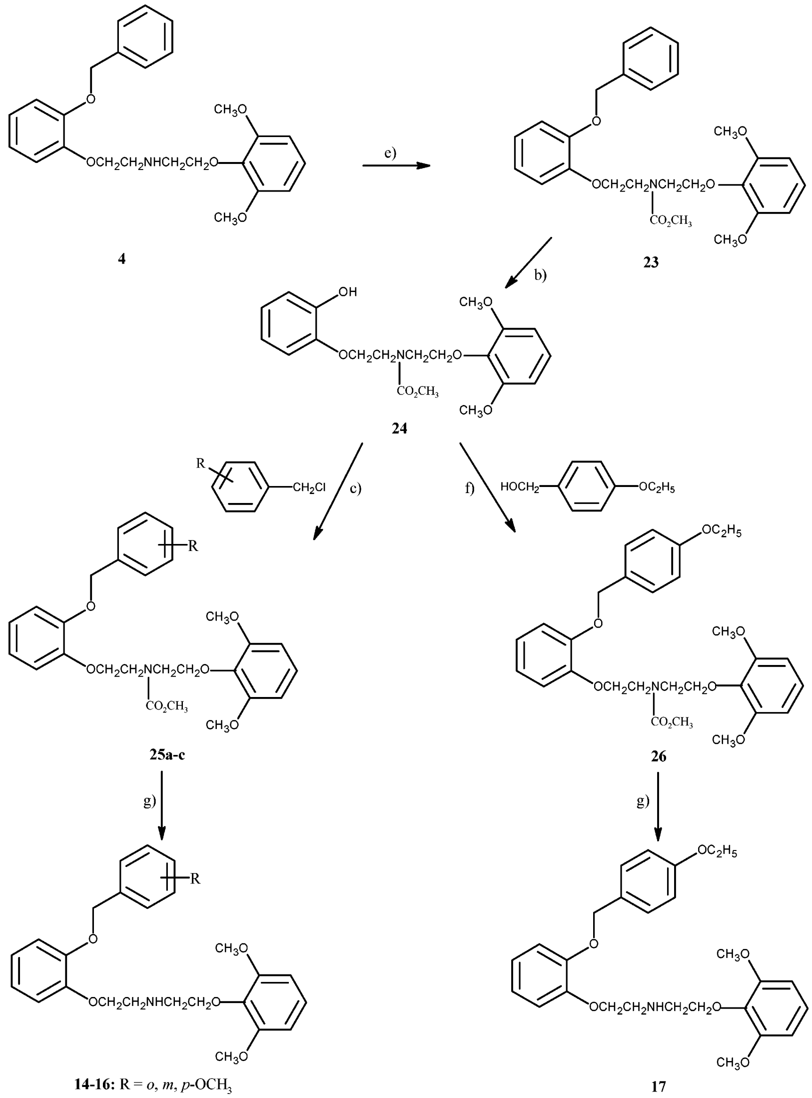

[a] Reagents: (b) H_2/Pd; (c) K_2CO_3/DMF; (e) MeOCOCl/Et_3N/$CHCl_3$; (f) DIAD/Ph_3P/THF; (g) KOH/MeOH.

rides. Subsequent acidic hydrolysis of the substituted benzyl ethers obtained (**21a**−**i**) yielded the corresponding aldehydes (**22a**−**i**), which produced compounds **5**−**13** by reductive amination with 2-(2,6-dimethoxyphenoxy)ethylamine[32] (Scheme 1). Since the acidic hydrolysis of *p*-alkoxy-substituted benzyl ethers afforded the corresponding aldehydes with very low yields, ligands **14**−**17** were prepared according to Scheme 2, starting from *N*-[2-[2-benzyloxyphenoxy]ethyl]-*N*-[2-(2,6-dimethoxyphenoxy)ethyl]amine (**4**).[26] Protection of the amino group with methyl chloroformate (compound **23**) and the subsequent catalytic cleavage of the benzyl group yielded the corresponding phenol (**24**), which was then alkylated with the appropriate benzyl chlorides in DMF and K_2CO_3 to obtain derivatives **25a**−**c**, or else etherified with *p*-ethoxybenzyl alcohol in the presence of DIAD and $(C_6H_5)_3P$ to give **26**. The basic hydrolysis of the carbamates **25a**−**c** and **26** thus obtained yielded the corresponding methoxy (**14**−**16**) and ethoxy (**17**) derivatives. Finally, compound **18** was prepared as shown in Scheme 3. (2-Hydroxyphenoxy)acetic acid methyl ester was alkylated with (4-isopropoxyphenyl)-methanol to the corresponding ester **27**, which was transformed into [2-(4-isopropoxybenzyloxy)phenoxy]acetic acid (**28**) by subsequent basic hydrolysis. Compound **28** was amidated in the presence of Et_3N and EtOCOCl with 2-(2,6-dimethoxyphenoxy)ethylamine[32] to the corresponding amide **29**, which was reduced with borane−methyl sulfide complex in dry THF to give compound **18**.

Results and Discussion

Binding and Functional Experiments. The pharmacological profile of compounds **5**−**16** was evaluated by radio-receptor binding assays and compared with **4**[26] and doxazosin[33] as reference compounds. [^{3}H]Prazosin was used to label cloned human α_1-AR subtypes expressed in CHO cells.[34] Furthermore, [^{3}H]8-hydroxy-2-(di-*n*-propylamino)tetralin was used to label cloned human serotonin 5-HT_{1A} receptors expressed in HeLa cells.[35] Affinity for the three α_1-AR subtypes and for the 5-HT_{1A} subtype was expressed as pK_i values and is shown in Table 1.

Receptor subtype selectivity of compounds **5**−**18** was further determined on α_1-ARs of different isolated tissues and compared with **4**[26] and doxazosin[33] as reference compounds. α_1-AR subtypes blocking activity was assessed by antagonism of (−)-NE-induced contrac-

Scheme 3[a]

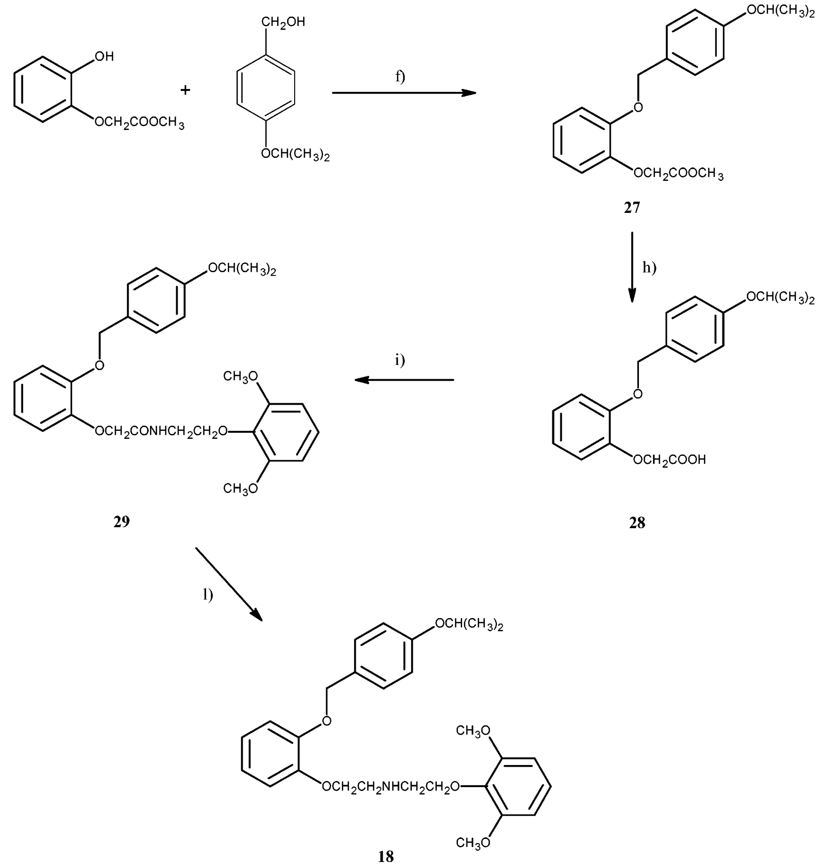

[a] Reagents: (f) DIAD/Ph_3P/THF; (h) NaOH; (i) EtOCOCl/Et_3N; 2-(2,6-dimethoxyphenoxy)ethylamine[32]/$CHCl_3$; (l) $BH_3 \cdot Me_2S$/THF.

tion of rat prostatic vas deferens (α_{1A})[36] or thoracic aorta (α_{1D})[37] and by antagonism of (−)-phenylephrine-induced contraction of rat spleen (α_{1B}).[38] The antagonist potency of the compounds, expressed as pK_B values,[39] is reported in Table 1.

The agonist efficacy of compounds **4**−**8**, **12**, **13**, and **16** toward 5-HT_{1A} receptors was assessed by determining the induced stimulation of [^{35}S]GTPγS binding in cell membranes from HeLa cells transfected with human cloned 5-HT_{1A} receptors,[40] and was expressed as pD_2 (−log ED_{50}) values (Table 1). ED_{50} represents the molar concentration of agonist, which produces 50% of the maximum possible response for that agonist.

The analysis of the results shows that all the compounds synthesized were potent α_1-AR antagonists, whose pK_B values observed in the functional experiments were comparable, in most cases, with the pK_i affinity derived from the binding assays; the latter were in any case higher than the former by 0.5 to 1.5 logarithmic units. Similarly to lead **4**,[26] all the new compounds generally displayed the highest affinity values at the α_{1D} subtype with respect to the other α_1-AR subtypes and to 5-HT_{1A}, at which all tested molecules behaved as partial agonists.

Attempts to improve the α_{1D}-affinity of **4** were made by inserting, into the ortho, meta, and para positions of the aromatic ring of the benzyloxy function, various substituents having different electronic, lipophilic, and steric contributions, and chosen using the Topliss approach.[29,30]

The first compound prepared was the *p*-chlorophenyl derivative (**7**). Since its potency was slightly lower but not significantly different from that of the unsubstituted-phenyl **4**, we decided to explore both branches of Topliss tree. So we also synthesized the *p*-methoxyphenyl derivative (**16**), whose α_{1D}-AR affinity was comparable to those of compounds **4** and **7**. Since the rank order of the substituents (*p*-Cl and *p*-OCH_3), with respect to activity, did not correspond completely to any parameter dependency, with the two substituents having opposite σ and π effects (*p*-OCH_3: -π, -σ; *p*-Cl: +π, +σ), synthesis proceeded under the branch of *p*-chlorophenyl **7** with the preparation of the *p*-methyl analogue **10**, whose substituent is a +π, -σ type. The equiactivity of **10** with respect to **7** led us to suppose that the expected increase of potency was hindered by steric reasons of the para substitution; thus, the next compound synthesized was the *m*-chloro derivative **6**, which represented the descending term both of *p*-chlorophenyl **7** in the central branch, and of *p*-methoxyphenyl **16** in the left branch of the Topliss operational scheme. Since also compound **6** showed an affinity value similar to that of lead compounds of both branches, the sequence was continued with the *m*-methyl derivative (compound **9**) and, subsequently, with the *o*-chloro-, *o*-methyl-, and *o*-methoxy-derivatives (compounds **5**, **8**, and **14**, respectively). Also these compounds did not significantly modify affinity for the α_{1D}-AR subtype. Therefore, the *p*-nitro analogue **13** was synthesized on the grounds that a +σ effect was operating, but that lower lipophilicity was optimal. Finally, compound **13** proved significantly more active than the preceding derivatives, even though it was equiactive with the unsubstituted lead compound **4**.

Table 1. Affinity Constants Expressed as pK_i (−log K_i) for Human Recombinant α_1-AR Subtypes and 5-HT_{1A} Receptors,[a] Affinity Constants Expressed as pK_B (−log K_B) at α_1-AR Subtypes on Isolated Tissues,[b] Agonist Efficacy ([^{35}S]GTPγS Binding) Expressed as pD_2 (−log ED_{50}) on 5-HT_{1A} Serotoninergic Receptors,[a] and Cytotoxic Activity[c] of Compounds **4−18**, in Comparison with Doxazosin

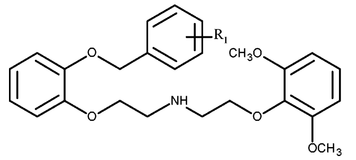

compd	R_1	pK_i cloned receptors (human brain) α_{1a}	α_{1b}	α_{1d}	pK_B isolated tissues α_{1A}	α_{1B}	α_{1D}	cloned 5-HT_{1A} receptors (human brain) pK_i	pD_2	% max	cytotoxic activity (human PC-3 prostate cancer cells) GI_{50} μM	TGI μM	LC_{50} μM
4	H	9.33[d]	9.27[d]	10.17[d]	8.39 ± 0.18[d]	8.30 ± 0.15	9.37 ± 0.15[d]	7.93	7.11	45.7	26.9 ± 1.2	76.9 ± 3.8	193.1 ± 9.3
5	*o*-Cl	8.85	9.25	9.60	8.56 ± 0.13	7.52 ± 0.09	8.59 ± 0.05	8.32	7.31	74.4	5.4 ± 0.2	17.8 ± 0.8	58.9 ± 2.9
6	*m*-Cl	9.60	9.80	10.3	8.12 ± 0.21	7.93 ± 0.22	8.72 ± 0.15	8.18	7.15	67.1	5.9 ± 0.3	20.4 ± 1.0	58.9 ± 3.4
7	*p*-Cl	9.60	9.00	10.5	8.17 ± 0.13	8.06 ± 0.06	9.11 ± 0.20	7.81	6.98	60.0	2.4 ± 0.1	14.5 ± 0.8	52.5 ± 2.9
8	*o*-CH_3	8.80	9.10	9.90	7.81 ± 0.02	7.67 ± 0.18	8.64 ± 0.20	7.95	6.96	75.6	11.5 ± 0.4	33.9 ± 1.3	*g*
9	*m*-CH_3	9.40	9.60	9.70	8.30 ± 0.16	8.20 ± 0.01	8.85 ± 0.10	7.74	*f*	*f*	12.0 ± 0.5	32.3 ± 1.4	87.1 ± 6.3
10	*p*-CH_3	8.70	9.60	10.20	8.23 ± 0.06	8.43 ± 0.18	9.12 ± 0.23	7.65	*f*	*f*	7.8 ± 0.5	27.5 ± 1.1	61.7 ± 3.0
11	*o*-NO_2	8.10	8.60	9.04	8.20 ± 0.06	8.56 ± 0.22	8.95 ± 0.01	7.62	*f*	*f*	13.2 ± 0.7	34.7 ± 1.3	95.5 ± 5.6
12	*m*-NO_2	9.50	9.10	10.20	8.85 ± 0.03	8.74 ± 0.18	9.28 ± 0.22	7.68	7.16	44.4	13.2 ± 0.6	38.9 ± 1.5	*g*
13	*p*-NO_2	8.90	9.40	10.30	8.58 ± 0.09	9.02 ± 0.12	9.41 ± 0.06	7.93	6.15	79.1	12.0 ± 0.6	43.6 ± 1.9	*g*
14	*o*-OMe	8.70	8.20	8.70	8.53 ± 0.14	8.13 ± 0.17	8.86 ± 0.13	7.63	*f*	*f*	8.9 ± 0.4	30.2 ± 1.5	100.0 ± 4.9
15	*m*-OMe	8.70	8.70	9.50	8.30 ± 0.05	8.31 ± 0.11	9.12 ± 0.21	7.51	*f*	*f*	2.5 ± 0.1	15.1 ± 1.0	61.7 ± 3.4
16	*p*-OMe	8.70	9.40	10.00	8.54 ± 0.07	9.51 ± 0.01	9.21 ± 0.19	7.76	7.92	21.6	8.5 ± 0.2	34.7 ± 1.2	*g*
17	*p*-OEt	*f*	*f*	*f*	8.50 ± 0.18	8.23 ± 0.19	9.11 ± 0.13	*f*	*f*	*f*	5.2 ± 0.3	18.2 ± 1.0	51.3 ± 2.7
18	*p*-O*i*Pr	*f*	*f*	*f*	8.17 ± 0.19	8.62 ± 0.11	9.14 ± 0.11	*f*	*f*	*f*	2.0 ± 0.1	17.8 ± 0.9	63.1 ± 3.0
Doxazosin	-	9.27[e]	9.09[e]	9.09[e]	8.69 ± 0.70[e]	9.51 ± 0.41[e]	8.97 ± 0.23[e]	*f*	*f*	*f*	26.9 ± 1.3	49.0 ± 2.5	75.8 ± 3.6

[a] Equilibrium dissociation constants (K_i) were derived from IC_{50} values using the Cheng−Prusoff equation.[51] The affinity estimates were derived from displacement of [^{3}H]prazosin for α_1-ARs, and [^{3}H]8-hydroxy-2-(di-*n*-propylamino)tetralin and [^{35}S]GTPγS binding for 5-HT_{1A} receptors (antagonism and agonism, respectively). Each experiment was performed in triplicate. K_i values were from two to three experiments, which agreed within ±20%. [b] α_1-AR subtypes blocking activity was assessed by antagonism of (−)-NE-induced contractions on isolated rat prostatic vas deferens (α_{1A})[36] or thoracic aorta (α_{1D})[37] and by antagonism of (−)-phenylephrine-induced contractions on rat spleen (α_{1B}).[38] pK_B values were calculated according to van Rossum[39] in the range of 0.01−1 μM. Each concentration [B] of antagonist was tested four times. [c] In vitro cytotoxic activity on human PC-3 prostate cancer cells was carried out by sulforhodamine B (SRB) assay, according to the National Cancer Institute protocol.[43] Growth Inhibition 50 (GI_{50}) represents the drug concentration (μM) required to inhibit 50% net of cell growth. Total growth inhibition (TGI) represents the drug concentration (μM) required to inhibit 100% of cell growth. Lethal concentration 50 (LC_{50}) represents the drug concentration required to kill 50% of the initial cell number. Each quoted value represents the mean of quadruplicate determinations ± standard error (n = 5). [d] Data from ref 26. [e] Data from ref 33. [f] Not determined. [g] Cytotoxicity activity < 50% net of cell growth.

Up to this point, the SAR studies at the benzyloxy moiety led to several compounds, which, even though modified with substituents having all the possible combinations of σ and π parameters, did not display any increase in the already high α_{1D}-affinity of lead compound **4**. The reason for this behavior can be found in an examination of the molecular complex that the antagonist **4** forms with the α_{1D}-AR subtype, as was recently described.[41] In fact, in this type of interaction, because of the high flexibility of the ligand, the benzyloxy function is buried in the core of the receptor helices bundle of the transmembrane domain, inside an area sterically accessible to the various substituent groups inserted in the aromatic ring. However, none of them is able to recognize additional binding sites: therefore, the main contribution to the binding energy, both in the case of **4** and for the whole series of derivatives **5−18**, is afforded by the strong hydrophobic interaction between the benzyloxy function of the ligand and the corresponding receptor site.

Neither did the α_{1A}-affinity potency draw any noticeable advantage from the introduction of substituents into the various positions of the aromatic ring; only the *m*-nitro derivative **12** showed slight improvement of affinity with a pK_B value of 8.85 compared with that of 8.39 of the reference compound **4**.

Instead, in the case of the α_{1B}-AR subtype, an interesting modulation of affinity was obtained: this drew advantage from the substitution of the nitro group and, in particular, when in the para position (compound **13**) (pK_B *o*-nitro derivative 8.56; *m*-nitro derivative 8.74; *p*-nitro derivative 9.02) and with the methoxy group exclusively in the para position (compound **16**) (pK_B *p*-methoxy derivative 9.51 against a value of 8.30 for prototype **4**). The increase of the α_{1B}-affinity, which cannot be attributed to electronic effect, in that the two groups mentioned above possess parameter values of opposite sign ($\sigma_{pOMe} = -0.27$, $\sigma_{pNO2} = +0.78$), is favored by the hydrophilic character ($\pi_{pOMe} = -0.02$, $\pi_{pNO2} = -0.28$) and by a definite steric hindrance ($MR_{pOMe} = 7.87$, $MR_{pNO2} = 7.36$). Lipophilic (Cl, CH_3, OC_2H_5, $OCHMe_2$) and more sterically hindered (OC_2H_5, $OCHMe_2$) substituents seem to negatively affect the α_{1B}-antagonist potency.

In Vitro Cytotoxic Activity. In vitro cytotoxic activity on human PC-3 prostate cancer cells of compounds **4−18** and doxazosin[42] for useful comparison, was carried out by sulforhodamine B (SRB) assay, according to the National Cancer Institute protocol.[43] The antitumor activity was estimated on the basis of measurements of three parameters: GI_{50}, the molar concentration of the compound that inhibits 50% net of cell growth; TGI, the molar concentration of the compound that causes total inhibition; and LC_{50}, the molar concentration of the compound causing 50% net of cell death. The new compounds **5−18** were active at low micromolar concentration and more effective than lead **4** in suppressing cell growth of PC-3 cells (Table 1).

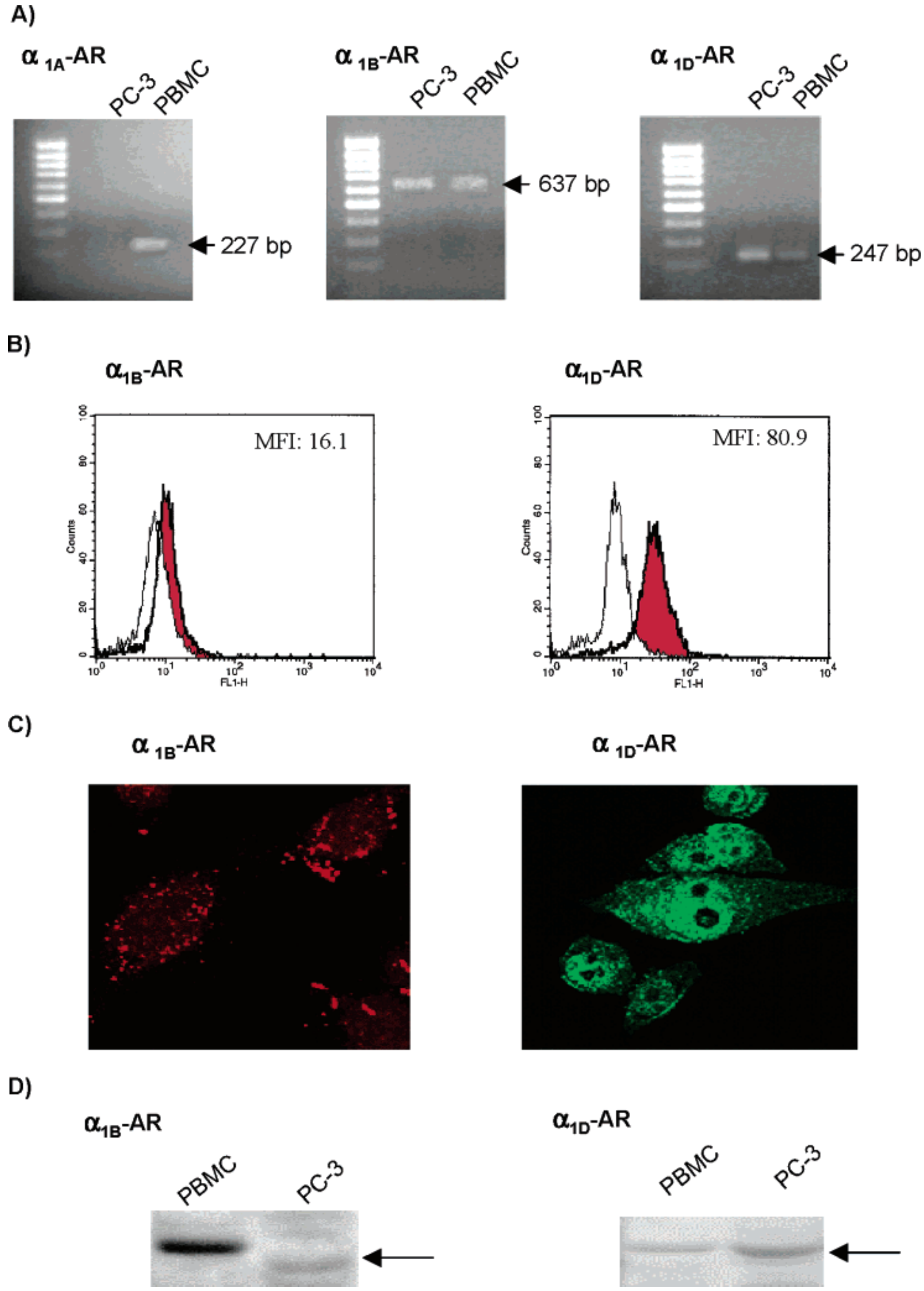

Figure 1. Expression of α_{1D}- and α_{1B}-AR subtypes in PC-3 cells. (A) α_{1A}-, α_{1B}-, and α_{1D}-AR subtypes mRNA expression in PC-3 cells and PBMC were evaluated by RT-PCR. PCR products were analyzed by 1.7% ethidium bromide-stained agarose gel and acquired using a Chemidoc (Bio-Rad). (B) The expression of α_{1B}- and α_{1D}-AR subtypes in PC-3 cells was evaluated by immunofluorescence and FACS analysis using a goat anti-α_{1B}-AR and a rabbit anti-α_{1D}-AR polyclonal Abs, respectively. FITC-conjugated RAG and FITC-conjugated GARB were used as secondary Abs. The data are expressed as mean fluorescence intensity (MFI); RAG = 2.94; GARB−FITC = 2.36. The white area indicates negative control; the red area indicates α_{1B}- or α_{1D}-AR positive cells. (C) Immunocytochemical localization of α_{1D}- and α_{1B}-AR subtypes in PC-3 cells was evaluated by confocal microscopy. Goat anti-α_{1B}-AR and rabbit anti-α_{1D}-AR polyclonal Abs were used as primary Abs; FITC-conjugated RAG and FITC-conjugated GARB were used as secondary Abs. Each image is the sum of one of three single optical sections taken at 1-μM intervals. Bars = 5 μM. (D) Lysates from PC-3 cells and human PBMC were separated on 8% SDS−PAGE and probed with a goat anti-α_{1B}-AR and a rabbit anti-α_{1D}-AR polyclonal Abs. Sizes are shown in kDa; the arrowhead indicates the band corresponding to α_{1B}- and α_{1D}-AR subtypes. All data shown are representative of three separate experiments.

Thus, the presence of a substituent in the benzyloxy moiety of these compounds seems to favor PC-3 cell growth inhibition, with **7** exhibiting potency (GI_{50} = 2.4 ± 0.1; TGI = 14.5 ± 0.08) significant higher than those of lead **4** (GI_{50} = 26.9 ± 1.2; TGI = 76.9 ± 3.8) and doxazosin (GI_{50} = 26.9 ± 1.3; TGI = 49 ± 2.5). Moreover, para substitution seems to improve growth inhibition activity. Concerning cytotoxic activity, **7** showed an effect higher (LC_{50} = 52.5 ± 2.9) than those of lead **4** and doxazosin (LC_{50} = 193.1 ± 9.3 and 75.8 ± 3.6, respectively). Compounds **8**, **12**, **13**, and **16** were devoid of cytotoxic activity. Finally, since serotonin has been reported to show an enhancing effect on human prostate cancer cells growth,[13] and **4**−**8**, **12**, **13**, and **16** are endowed with a 5-HT_{1A} partial agonist activity, the effect of these compounds on PC-3 cell growth also in the presence of the 5-HT_{1A} antagonist, (*S*)-WAY 100135, was evaluated. In these experiments, (*S*)-WAY 100135, neither alone nor in combination with **4**, **7**, or doxazosin reversed the inhibitory effects induced by compounds **4**, **7**, or doxazosin on PC-3 cell growth (data not shown).

Expression of α_1-AR Subtypes in PC-3 Cells. To directly demonstrate the α_1-AR subtypes mRNA expression in PC-3 ($p53^{-/-}$) human androgen-nonresponsive prostate cancer cells, a qualitative PCR analysis on PC-3 cells and human peripheral blood mononuclear cells (PBMC), used as positive control, was performed. Our results indicated that α_{1B}- and α_{1D}-AR subtypes mRNAs were expressed in PC-3 cells and PBMC, as shown by the finding of PCR products of expected size, [637 bp (α_{1B}-AR) and 247 bp (α_{1D}-AR), respectively]. As previously reported,[8] no α_{1A}-AR mRNA expression was detected in PC-3 cells (Figure 1A). The expression of α_{1B}-AR and α_{1D}-AR subtypes in PC-3 cells was also assessed at protein level. Immunofluorescence and FACS analysis showed that these cells expressed high levels of α_{1D}-AR protein (MFI = 80.9), whereas lower expression (MFI = 16.1) was observed for the α_{1B}-AR protein (Figure 1B). Confocal microscopy analysis showed that α_{1B}-AR subtype was localized near the plasma membrane of PC-3 cells, whereas a broader expression of α_{1D}-AR on the plasma membrane, cytosol, and nucleus was found (Figure 1C).

Moreover, Western blot analysis of cell lysates revealed a band with an apparent MW of about 56 kDa, and a band of 70 kDa (Figure 1D), likely corresponding to the α_{1B}- and α_{1D}-AR subtypes, respectively; similar bands were also evident in the lysates from human PBMC used as positive control. No reactivity was observed with normal goat serum and with normal rabbit serum used as negative control (data not shown). Taken together, these results demonstrate for the first time the expression of the α_{1B}- and α_{1D}-AR subtypes on human PC-3 cells, both at mRNA and protein levels.

Apoptotic Activity. A characteristic feature of apoptotic cell death is the loss of phospholipid asymmetry and expression of phosphatidylserine (PS) on the outer layer of the plasma membrane.[44] Thus, we analyzed whether the treatment of PC-3 cells with the new antagonist **7**, selected for its interesting biological profile, and the lead compound **4** induced externalization of PS residues from the inner to the outer leaflet of the plasma membrane in these cells and consequently increased the Annexin V binding. Since doxazosin has been proved to induce apoptosis of PC-3 cells,[8,10] it was used as positive control. Exposure of PC-3 cells to compounds **7** and **4** resulted in a time- and dose-dependent reduction of cell viability and induction of apoptotic cell death. Compound **7** showed the highest potency to affect PC-3 cell viability and to induce apoptosis (Figure 2A-B). Although PC-3 cells were susceptible to compound **4**- or doxazosin-induced apoptosis at 50 μM, very low and no appreciable apoptotic death was evaluated at 10 μM with compound **4** and doxazosin, respectively.

Finally, once the expression of α_{1B}- and α_{1D}-AR subtypes on PC-3 cells was observed, we analyzed whether the proapoptotic effect induced by treatment with **7** and **4**, resulted in a dose-dependent modulation of α_{1B}- and α_{1D}-AR expression on PC-3 cells. As shown in Figure 3A, treatment of PC-3 cells with **7** and **4** induced a marked reduction of α_{1D}-AR expression, with antagonist **7** showing the highest inhibitory effect (MFI from 80.9 to 21.5 at 50 μM concentration). Doxazosin used at 50 μM showed the lowest ability to affect α_{1D}-AR expression. Compounds **7** and, partially, **4** affect, mainly at higher dose, the α_{1B}-AR expression on PC-3 cells, whereas doxazosin did not show any significant effect at either of the dose used (Figure 3B).

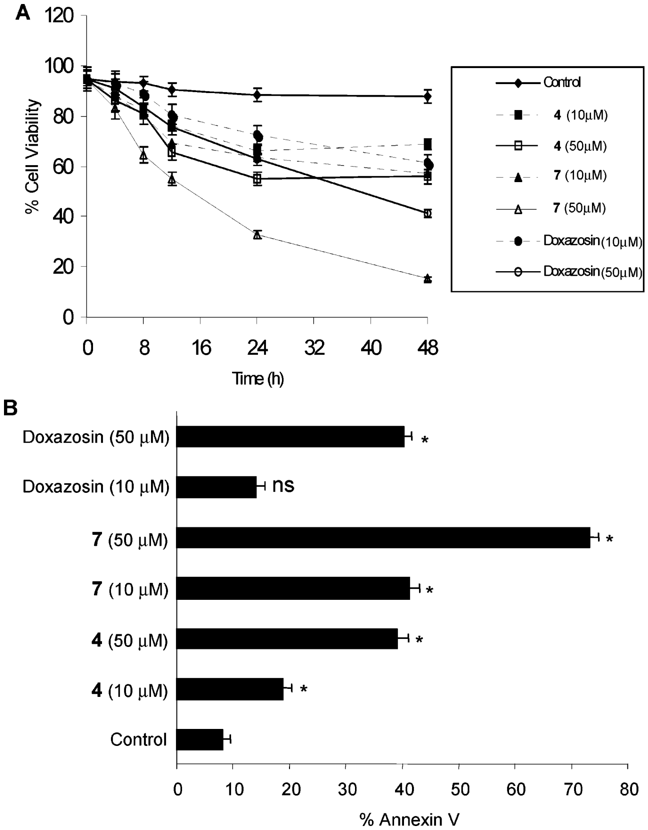

Figure 2. α_1-AR antagonists affect cell viability and induce PS exposure in PC-3 cells. (A) Cell viability of PC-3 cells, treated with different doses (10 and 50 μM) of **7**, lead **4** and doxazosin for 24 h at 37 °C, was evaluated by PI staining and cytofluorimetric analysis. Data are representative of one of three separate experiments. (B) The expression of Annexin V on PC-3 cells, treated with 50 μM of **7**, lead **4**, and doxazosin, was evaluated by immunofluorescence and FACS analysis. Data are the mean ± SD of three separate experiments. Statistical analysis was determined by comparing the MFI from untreated with **4**-, **7**-, and doxazosin (10 and 50 μM)-treated PC-3 cells. *$P < 0.01$ determined by Student's *t*-test. ns = Not significant comparing the MFI from untreated with doxazosin (10 μM)-treated PC-3 cells.

Overall, these results indicate that the apoptosis triggered by the α_1-AR antagonists **7** and **4** is associated with a significant reduction of α_{1D}-AR and α_{1B}-AR subtypes in PC-3 positive cells, suggesting a role for these AR subtypes in the modulation of apoptosis.

NE Protects PC-3 Cells from α_1-AR Antagonist-Induced Apoptosis. NE has been shown to promote survival in different cell types by acting as endogenous modulator of cell death.[45−47] Thus, the ability of the endogenous agonist NE, used at different concentrations (10 and 50 μM), to reverse the α_1-AR antagonist (50 μM)-induced inhibitory effects on PC-3 cells has been evalu-

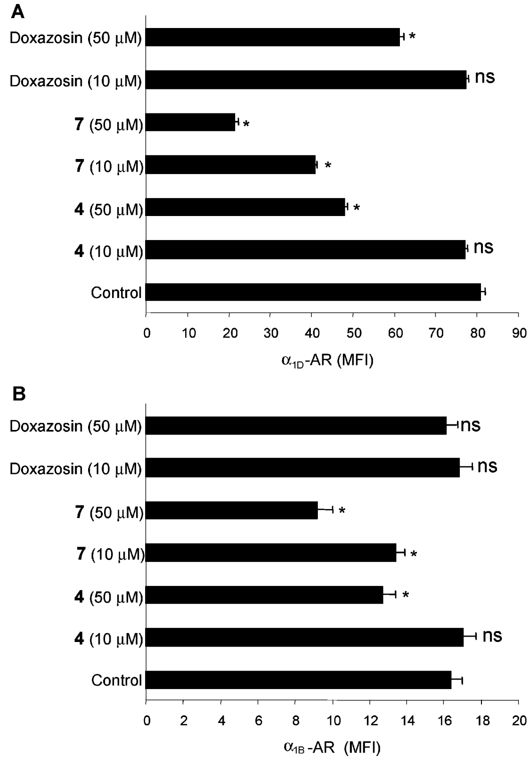

Figure 3. α_1-AR antagonists treatment modulates α_{1D}- and α_{1B}-AR expression in PC-3 cells. The expression of α_{1D}- (panel A) and α_{1B}-AR (panel B) subtypes in PC-3 cells, treated with different concentrations (10 and 50 μM) of **7**, lead **4**, and doxazosin, was evaluated by immunofluorescence and FACS analysis as described above. The data shown represent the mean ± SD of three separate experiments and are expressed as mean MFI. Statistical analysis was determined by comparing the MFI from untreated with **4**-, **7**-, and doxazosin (10 and 50 μM)-treated PC-3 cells. *$P < 0.01$ determined by Student's *t*-test. ns = Not significant comparing the MFI from untreated with **4**- (10 μM)- and doxazosin (10 and 50 μM)-treated PC-3 cells.

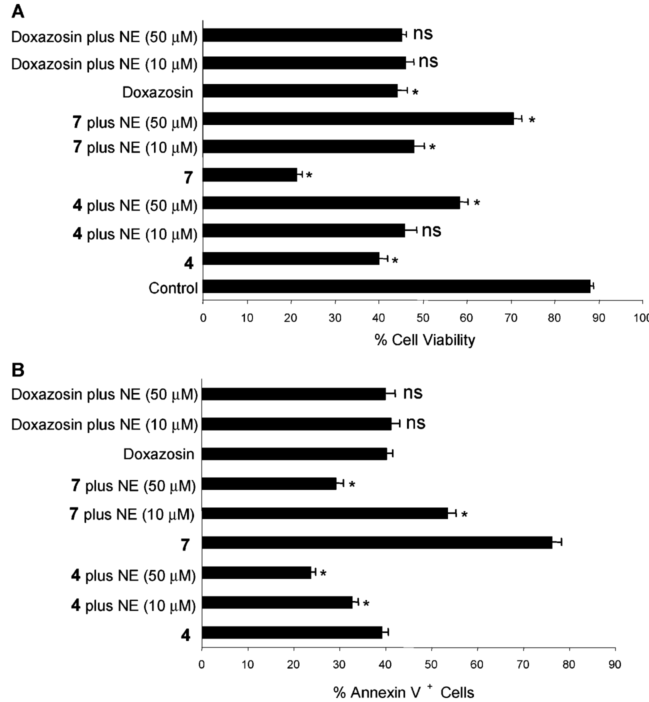

Figure 4. NE protects PC-3 cells from α_1-AR antagonist-induced apoptosis. (A) Cell viability of PC-3 cells treated with 50 μM of **7**, lead **4**, and doxazosin for 24 h at 37 °C, alone or in combination with different doses (10 and 50 μM) of NE, was evaluated by PI staining and cytofluorimetric analysis. Data are the mean ± SD of three separate experiments. Statistical analysis was determined by comparing the percentage of PI^+ cells from **4**-, **7**-, and doxazosin-treated with NE (10 and 50 μM) plus **4**, **7**, and doxazosin coadministered PC-3 cells. *$P < 0.01$ determined by Student's *t*-test. (B) The expression of Annexin V on PC-3 cells treated with **7**, lead **4**, and doxazosin (50 μM), alone or in combination with different doses of NE (10 and 50 μM), was evaluated by immunofluorescence and FACS analysis. Data are the mean ± SD of three separate experiments. Statistical analysis was determined by comparing the percentage of cell viability or Annexin V^+ cells from **4**-, **7**-, and doxazosin-treated with NE-treated (10 and 50 μM) plus **4**, **7**, and doxazosin coadministered PC-3 cells. *$P < 0.01$ determined by Student's *t*-test. ns = Not significant comparing the percent of cell viability from **4**- (10 μM)-treated with NE-treated (10 μM) plus **4**, and the percentage of cell viability or Annexin V^+ cells from doxazosin-treated with NE-treated (10 and 50 μM) plus doxazosin coadministered PC-3 cells.

ated. NE markedly protected PC-3 cells from α_1-AR antagonist-dependent apoptosis and completely reversed in a dose-dependent manner the reduction of PC-3 cell viability (Figure 4A) and apoptosis (Figure 4B) induced by **7**, and, to a lesser extent, by exposure to **4**. On the other hand, treatment with NE did not affect the ability of doxazosin to inhibit cell viability and to induce apoptosis of PC-3 cells.

As reported in Figure 5A,B, NE (10 and 50 μM) significantly increased in a dose-dependent manner the expression of α_{1D}-AR and, at 50 μM, the expression of α_{1B}-AR on PC-3 cells. Moreover, treatment with NE completely reversed the reduction of α_{1D}- and α_{1B}-AR expression induced by **7** on PC-3 cells; it also reversed that of α_{1D}-AR expression induced by exposure to **4**, whereas it did not affect that of α_{1B}-AR subtype expression. Finally, it did not reverse the inhibitory effect of doxazosin on the α_{1D}-AR subtype expression in PC-3 cells.

NE Stimulates PC-3 Cell Proliferation. Given the growing evidence on the role of α_1-ARs in the direct mitogenic effect of catecholamines on prostate growth,[7,20] we examined whether the protective effects, induced by NE on α_1-AR positive PC-3 cells, were partially related to its ability to induce PC-3 cell proliferation. Thus, the effect of NE, at different doses (0, 0.1, 1, 10, and 50 μM), to stimulate PC-3 cell proliferation was evaluated by BrdU incorporation into the DNA of proliferating cells using a colorimetric ELISA kit. NE markedly enhanced in a dose-dependent manner (10 μM = 33% and 50 μM = 65%) PC-3 cell proliferation. Moreover, the new antagonist **7** (0.5 μM), and, to a lesser extent, the lead **4** (1.0 μM), but not doxazosin (1.0 μM), completely inhibited the NE-induced increase of PC-3 cell proliferation (Figure 6).

Conclusions

The present study, for the first time, highlights the expression of α_{1D}- and α_{1B}-AR subtypes in human androgen nonresponsive PC-3 prostate cancer cells. Interestingly, α_{1D}-AR seems to be predominantly located in intracellular vescicles, which are widespread in the cytosol and nucleus, while the majority of the α_{1B}-AR is clustered around the plasma membrane of PC-3 cells. The α_{1D}-AR subtype is a phosphoprotein whose function

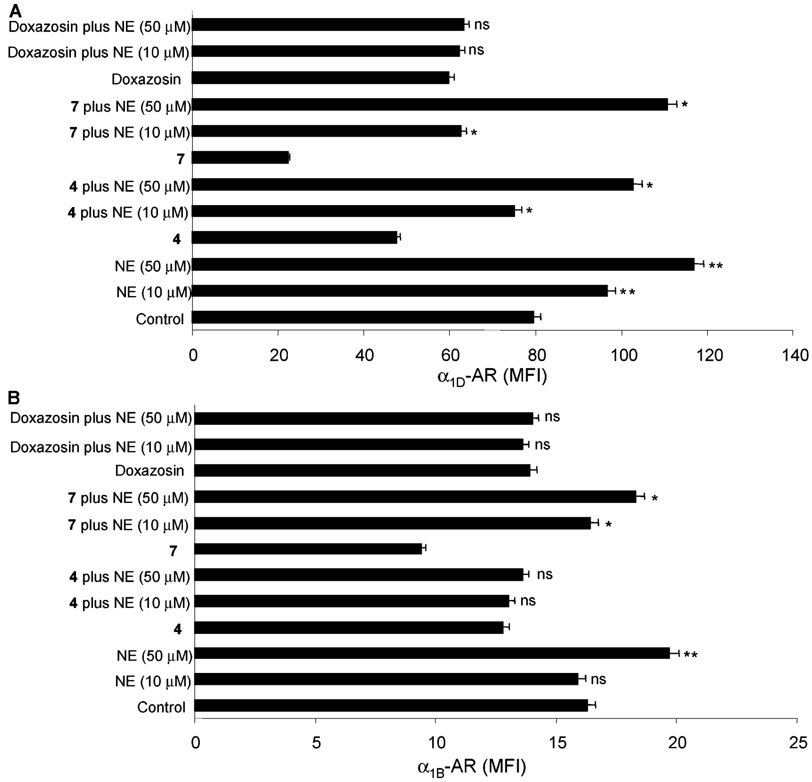

Figure 5. NE increases the expression of α_{1D}- and α_{1B}-AR subtypes in untreated, NE- and α_1-AR antagonists-treated PC-3 cells. The expression of α_{1D}- and α_{1B}-AR subtypes in PC-3 cells, untreated, treated with different doses of NE (10 and 50 μM), or with **7**, lead **4**, and doxazosin, alone or in combination with different doses (10 and 50 μM) of NE, was evaluated by immunofluorescence and FACS analysis as described above. The data shown represent the mean ± SD of three separate experiments and are expressed as MFI. Statistical analysis was determined by comparing the MFI of α_{1D}- and α_{1B}-AR subtypes positive cells, from untreated and NE-treated (10 and 50 μM) (**$P < 0.01$) and **4**-, **7**-, and doxazosin-treated with that of NE (10 and 50 μM) plus **4**, **7**, and doxazosin coadministered PC-3 cells. *$P < 0.01$ determined by Student's *t*-test.

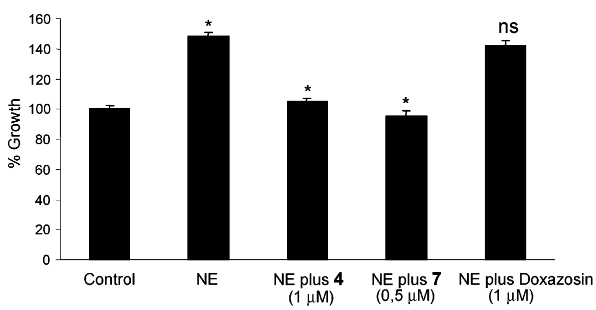

Figure 6. Lead **4** and **7** (1 and 0.5 μM), but not doxazosin (1 μM), treatment inhibits NE (50 μM)-induced increase of PC-3 cell proliferation, as evaluated by immunoassay using cell proliferation ELISA BrdU. Data are the mean ± SD of three separate experiments. Statistical analysis was determined by comparing the percentage of growth from untreated with NE-treated, and NE with NE plus **4**, **7**, and doxazosin (1, 0.5, and 1 μM, respectively) coadministered PC-3 cells. *$P < 0.01$ determined by Student's *t*-test. ns = Not significant comparing the percentage of growth from NE with NE plus doxazosin (1 μM) coadministered PC-3 cells.

is regulated through phosphorylation, so that its intracellular localization could be the result of its intrinsic activity, which could trigger phosphorylation and internalization. On the other hand, the presence of α_{1B}-AR near the plasma membrane may support its ability to act as a chaperon for the proper insertion of α_{1D}-AR in the plasma membrane.[48,49]

We also demonstrate the involvement of these receptors in the regulation of apoptosis and cell proliferation. Thus, **7**- and **4**-induced apoptosis is associated with a significant reduction of α_{1D}- and α_{1B}-AR expression in PC-3 cells. NE markedly protects, in a dose-dependent manner, PC-3 cells from apoptosis induced by these α_1-AR antagonists and completely reverses the depletion of α_{1D}-AR and α_{1B}-AR PC-3 positive cells induced by treatment with **7**. Moreover, our study provides evidence that NE promotes the proliferation of PC-3 cells. The specificity of NE-induced proliferation is proven by its complete suppression by **7** and, at higher concentration, by **4**. Compound **7** also shows higher potency, with respect to **4**, to induce apoptosis. The high α_1-AR antagonist potency, the more significant α_{1D}-selectivity and the higher lipophilic character with respect to doxazosin might be the factors responsible for the effects evoked by **7**. Moreover, it is known that α_{1D}-AR forms heterodimers with the α_{1B}-AR subtype, and that such association may have consequences in their pharmacological properties and their function/regulation.[50] Thus, these effects may be related to the ability of **7** and, to a lesser extent, of **4**, to affect both α_{1D}-AR and α_{1B}-AR PC-3 cell populations.

In conclusion, clopenphendioxan (**7**) may represent a valid pharmacological tool and promising lead to design new ligands useful for prostate cancer treatment. Further studies have already been planned with the aim to obtain structurally optimized antagonists. The difference between interaction of the novel antagonists and doxazosin with NE is interesting and may warrant further investigation with other agonists and antagonists.

Experimental Protocols

Chemistry. Melting points were taken in glass capillary tubes on a Büchi SMP-20 apparatus and are uncorrected. IR and NMR spectra were recorded on Perkin-Elmer 297 and Varian EM-390 instruments, respectively. Chemical shifts are reported in parts per million (ppm) relative to tetramethylsilane (TMS), and spin multiplicities are given as s (singlet), d (doublet), t (triplet), q (quartet), or m (multiplet). IR spectral data (not shown because of the lack of unusual features) were obtained for all compounds reported and are consistent with the assigned structures. The microanalyses were performed by the Microanalytical Laboratory of our department. The elemental composition of the compounds agreed to within ±0.4% of the calculated value. Chromatographic separations were performed on silica gel columns (Kieselgel 40, 0.040–0.063 mm, Merck) by flash chromatography. The term "dried" refers to the use of anhydrous sodium sulfate. Compounds were named following IUPAC rules as applied by Beilstein-Institut AutoNom (version 2.1), a software for systematic names in organic chemistry.

(2-Benzyloxyphenoxy)acetaldehyde Dimethyl Acetale (19). A 60% NaH dispersion in mineral oil (0.22 g, 5.5 mmol) was washed with hexane under nitrogen, suspended in dimethylformamide (DMF; 0.7 mL), and then, after 30 min, added with a solution of 2-benzyloxyphenol (1.0 g; 4.99 mmol) in dry DMF (0.5 mL). The mixture was stirred at room temperature for 1.5 h and cooled to 0 °C. A solution of 2-chloro-1,1-dimethoxyethane (0.65 mL; 5.7 mmol) in DMF (8.0 mL) was added, and the reaction mixture was heated at 120 °C for 8 h. After cooling, the mixture was poured in 2 N NaOH (15 mL) and extracted with Et_2O. Removal of dried solvents gave a residue, which was purified by column chromatography. Eluting with cyclohexane/AcOEt (98:2) gave an oil; 0.85 g (59% yield). ^{1}H NMR ($CDCl_3$) δ 3.43 (s, 6, OCH_3), 4.07 (d, 2, OCH_2), 4.73 (t, 1, CH), 5.11 (s, 2, CH_2Ar), 6.88–7.48 (m, 9, ArH).

2-(2,2-Dimethoxyethoxy)phenol (20). A solution of **19** (0.5 g; 1.73 mmol) in AcOEt/AcOH (9:1; 4.3 mL) was hydrogenated over 10% Pd on charcoal (0.05 g) for 4 h at 50 psi of pressure. Following catalyst removal, the solution was diluted with Et_2O, and the extracts were washed with $NaHCO_3$ and ice. Removal of dried solvent gave an oil, which was purified by column chromatography. Eluting with cyclohexane/AcOEt (8:2) gave an oil; 0.3 g (87% yield). ^{1}H NMR ($CDCl_3$) δ 3.42 (s, 6, OCH_3), 4.02 (d, 2, OCH_2), 4.68 (t, 1, CH), 6.19 (br s, 1, OH), 6.76–6.94 (m, 4, ArH).

1-(2,2-Dimethoxyethoxy)-2-[(2-chlorobenzyl)oxy]benzene (21a). A mixture of **20** (0.6 g; 3.01 mmol), 2-chlorobenzyl chloride (0.57 mL; 4.51 mmol), and K_2CO_3 (0.42 g; 3.01 mmol) in DMF (6 mL) was refluxed for 45 min at 125 °C. After cooling to 0 °C, a solution of 5% NaOH was added and the solution was extracted with Et_2O.The extracts were washed with 5% NaOH and H_2O. Removal of dried solvent gave a residue, which was purified by column chromatography. Eluting with cyclohexane/AcOEt (9:1) gave an oil; 0.78 g (80% yield). ^{1}H NMR ($CDCl_3$) δ 3.48 (s, 6, OCH_3), 4.10 (d, 2, OCH_2), 4.78 (t, 1, CH), 5.23 (s, 2, CH_2Ar), 6.91–7.72 (m, 8, ArH).

Similarly, compounds **21b–i** were obtained via the procedure described for **21a**.

1-(2,2-Dimethoxyethoxy)-2-[(3-chlorobenzyl)oxy]benzene (21b). Eluting solvent: cyclohexane/AcOEt (9:1); 73% yield. ^{1}H NMR ($CDCl_3$) δ 3.44 (s, 6, OCH_3), 4.05 (d, 2, OCH_2), 4.68 (t, 1, CH), 5.09 (s, 2, CH_2Ar), 6.81–7.62 (m, 8, ArH).

1-(2,2-Dimethoxyethoxy)-2-[(4-chlorobenzyl)oxy]benzene (21c). Eluting solvent: cyclohexane/AcOEt (9.8:0.2); 53% yield. ^{1}H NMR ($CDCl_3$) δ 3.42 (s, 6, OCH_3), 4.02 (d, 2, OCH_2), 4.73 (t, 1, CH), 5.08 (s, 2, CH_2Ar), 6.88–7.42 (m, 8, ArH).

1-(2,2-Dimethoxyethoxy)-2-[(2-methylbenzyl)oxy]benzene (21d). Eluting solvent: cyclohexane/AcOEt (9.5:0.5); 63% yield. ^{1}H NMR ($CDCl_3$) δ 2.42 (s, 3, CH_3), 3.42 (s, 6, OCH_3), 4.07 (d, 2, OCH_2), 4.73 (t, 1, CH), 5.12 (s, 2, CH_2Ar), 6.93–7.52 (m, 8, ArH).

1-(2,2-Dimethoxyethoxy)-2-[(3-methylbenzyl)oxy]benzene (21e). Eluting solvent: cyclohexane/AcOEt (9:1); 77% yield. ^{1}H NMR ($CDCl_3$) δ 2.37 (s, 3, CH_3), 3.46 (s, 6, OCH_3), 4.06 (d, 2, OCH_2), 4.75 (t, 1, CH), 5.09 (s, 2, CH_2Ar), 6.83–7.43 (m, 8, ArH).

1-(2,2-Dimethoxyethoxy)-2-[(4-methylbenzyl)oxy]benzene (21f). Eluting solvent: cyclohexane/AcOEt (9.5:0.5); 82% yield. ^{1}H NMR ($CDCl_3$) δ 2.38 (s, 3, CH_3), 3.47 (s, 6, OCH_3), 4.09 (d, 2, OCH_2), 4.77 (t, 1, CH), 5.10 (s, 2, CH_2Ar), 6.88–7.40 (m, 8, ArH).

1-(2,2-Dimethoxyethoxy)-2-[(2-nitrobenzyl)oxy]benzene (21g). Eluting solvent: cyclohexane/AcOEt (9.5:0.5); 37% yield. ^{1}H NMR ($CDCl_3$) δ 3.44 (s, 6, OCH_3), 4.10 (d, 2, OCH_2), 4.80 (t, 1, CH), 5.55 (s, 2, CH_2Ar), 6.95–8.22 (m, 8, ArH).

1-(2,2-Dimethoxyethoxy)-2-[(3-nitrobenzyl)oxy]benzene (21h). Eluting solvent: cyclohexane/AcOEt (9:1); 60% yield; crystallized from AcOEt/petroleum ether, mp 86–87 °C. ^{1}H NMR ($CDCl_3$) δ 3.50 (s, 6, OCH_3), 4.10 (d, 2, OCH_2), 4.82 (t, 1, CH), 5.22 (s, 2, CH_2Ar), 6.90–8.42 (m, 8, ArH).

1-(2,2-Dimethoxyethoxy)-2-[(4-nitrobenzyl)oxy]benzene (21i). Eluting solvent: cyclohexane/AcOEt (9:1); 30% yield; crystallized from AcOEt/petroleum ether, mp 106–107 °C. ^{1}H NMR ($CDCl_3$) δ 3.48 (s, 6, OCH_3), 4.10 (d, 2, OCH_2), 4.79 (t, 1, CH), 5.23 (s, 2, CH_2Ar), 6.90–8.26 (m, 8, ArH).

[2-(2-Chlorobenzyloxy)phenoxy]acetaldehyde (22a). Compound **21a** (0.78 g; 2.42 mmol) was added to a solution of 2 N HCl (3.9 mL) in acetone (6.7 mL), and the resulting solution was refluxed for 1.5 h with stirring. After cooling to 0 °C, Et_2O (25 mL) and H_2O (10 mL) were added. The ether layer was separated and washed with 5% Na_2CO_3 (1 × 25 mL) and H_2O (2 × 25 mL). Removal of dried solvent gave a residue, which was purified by column chromatography. Eluting with cyclohexane/AcOEt (8:2) gave a solid; 0.57 g (85% yield); mp 59–60 °C. ^{1}H NMR ($CDCl_3$) δ 4.63 (d, 2, OCH_2), 5.26 (s, 2, CH_2Ar), 6.83–7.63 (m, 8, ArH), 9.92 (t, 1, CHO).

Similarly, compounds **22b–i** were obtained via the procedure described for **22a**.

[2-(3-Chlorobenzyloxy)phenoxy]acetaldehyde (22b). Eluting solvent: cyclohexane/AcOEt (8:2); 67% yield. ^{1}H NMR ($CDCl_3$) δ 4.61 (d, 2, OCH_2), 5.10 (s, 2, CH_2Ar), 6.58–7.24 (m, 8, ArH), 9.84 (t, 1, CHO).

[2-(4-Chlorobenzyloxy)phenoxy]acetaldehyde (22c). 72% Yield. ^{1}H NMR ($CDCl_3$) δ 4.60 (d, 2, OCH_2), 5.09 (s, 2, CH_2Ar), 6.81–7.38 (m, 8, ArH), 9.84 (t, 1, CHO). This compound was used in the next step without further purification.

[2-(2-Methylbenzyloxy)phenoxy]acetaldehyde (22d). 71% Yield. ^{1}H NMR ($CDCl_3$) δ 2.42 (s, 3, CH_3), 4.60 (d, 2, OCH_2), 5.14 (s, 2, CH_2Ar), 6.61–7.44 (m, 8, ArH), 9.88 (t, 1, CHO). This compound was used in the next step without further purification.

[2-(3-Methylbenzyloxy)phenoxy]acetaldehyde (22e). Eluting solvent: cyclohexane/AcOEt (8:2); 72% yield. ^{1}H NMR ($CDCl_3$) δ 2.40 (s, 3, CH_3), 4.62 (d, 2, OCH_2), 5.12 (s, 2, CH_2Ar), 6.79–7.34 (m, 8, ArH), 9.90 (t, 1, CHO).

[2-(4-Methylbenzyloxy)phenoxy]acetaldehyde (22f). Eluting solvent: cyclohexane/AcOEt (8:2); 96% yield. ^{1}H NMR ($CDCl_3$) δ 2.39 (s, 3, CH_3), 4.59 (d, 2, OCH_2), 5.13 (s, 2, CH_2Ar), 6.70–7.38 (m, 8, ArH), 9.85 (t, 1, CHO).

[2-(2-Nitrobenzyloxy)phenoxy]acetaldehyde (22g). Eluting solvent: cyclohexane/AcOEt (8:2); 85% yield. ^{1}H NMR ($CDCl_3$) δ 4.15 (d, 2, OCH_2), 5.53 (s, 2, CH_2Ar), 6.82–8.22 (m, 8, ArH), 9.93 (t, 1, CHO).

[2-(3-Nitrobenzyloxy)phenoxy]acetaldehyde (22h). Eluting solvent: cyclohexane/AcOEt (8:2); 42% yield. ^{1}H NMR ($CDCl_3$) δ 4.10 (d, 2, OCH_2), 5.21 (s, 2, CH_2Ar), 6.84–8.25 (m, 8, ArH), 9.85 (t, 1, CHO).

[2-(4-Nitrobenzyloxy)phenoxy]acetaldehyde (22i). Eluting solvent: cyclohexane/AcOEt (8:2); 75% yield; mp 81–82 °C. ^{1}H NMR ($CDCl_3$) δ 4.12 (d, 2, OCH_2), 5.23 (s, 2, CH_2Ar), 6.84–8.24 (m, 8, ArH), 9.92 (t, 1, CHO).

{2-[2-(2-Chlorobenzyloxy)phenoxy]ethyl}-[2-(2,6-dimethoxyphenoxy)ethyl]amine (5). A 2 M solution of HCl gas in EtOH (1.55 mL) was added to a solution of 2-(2,6-dimethoxyphenoxy)ethylamine[32] (1.82 g; 9.23 mmol) and **22a** (0.43 g; 1.55 mmol) in EtOH (12.0 mL), followed by the addition of $NaBH_3CN$ (0.085 g; 1.35 mmol) and molecular sieves (4 Å). The mixture was stirred at room temperature for 1 h, then acidified at pH 1 with 2 N HCl, filtered, and evaporated. The residue was taken up with water and basified with 6 N NaOH, and the mixture was extracted with Et_2O. Removal of dried solvent gave a residue, which was purified by column chromatography. Eluting with $CHCl_3$/EtOH (9.8:0.2) gave **5** as the free base; 0.27 g (38% yield). ^1H NMR ($CDCl_3$) δ 1.88 (br s, 1, NH, exchangeable with D_2O), 2.99 and 3.12 (two t, 4, CH_2NCH_2), 3.81 (s, 6, OCH_3), 4.18 (m, 4, OCH_2 and CH_2O), 5.22 (s, 2, CH_2Ar), 6.53−7.64 (m, 11, ArH).

The free base was transformed into the oxalate salt by treating an ether solution with oxalic acid; the solid was crystallized from EtOH; mp 164−165 °C. Anal. ($C_{25}H_{28}ClNO_5 \cdot H_2C_2O_4 \cdot 0.5H_2O$) C, H, N.

Similarly, compounds **6**−**13** were obtained via the procedure described for **5**.

{2-[2-(3-Chlorobenzyloxy)phenoxy]ethyl}-[2-(2,6-dimethoxyphenoxy)ethyl]amine (6). Eluting with $CHCl_3$/EtOH (9.5:0.5) gave **6** as the free base; (45% yield). ^1H NMR ($CDCl_3$) δ 2.47 (br s, 1, NH, exchangeable with D_2O), 2.94 and 3.10 (two t, 4, CH_2NCH_2), 3.78 (s, 6, OCH_3), 4.13 (m, 4, OCH_2 and CH_2O), 5.06 (s, 2, CH_2Ar), 6.60−7.41 (m, 11, ArH). The oxalate salt was crystallized from EtOH; mp 135−136 °C. Anal. ($C_{25}H_{28}ClNO_5 \cdot H_2C_2O_4 \cdot 0.5H_2O$) C, H, N.

{2-[2-(4-Chlorobenzyloxy)phenoxy]ethyl}-[2-(2,6-dimethoxyphenoxy)ethyl]amine (7). Eluting with AcOEt/EtOH (9:1) gave **7** as the free base; (28% yield). ^1H NMR ($CDCl_3$) δ 2.15 (br s, 1, NH, exchangeable with D_2O), 2.95 and 3.08 (two t, 4, CH_2NCH_2), 3.77 (s, 6, OCH_3), 4.13 (m, 4, OCH_2 and CH_2O), 5.03 (s, 2, CH_2Ar), 6.49−7.34 (m, 11, ArH). The oxalate salt was crystallized from EtOH; mp 161−162 °C. Anal. ($C_{25}H_{28}ClNO_5 \cdot H_2C_2O_4 \cdot 0.5H_2O$) C, H, N.

[2-(2,6-Dimethoxyphenoxy)ethyl]-{2-[2-(2-methylbenzyloxy)phenoxy]ethyl}amine (8). Eluting with $CHCl_3$/EtOH (9.9:0.1) gave **8** as the free base; (28% yield). ^1H NMR ($CDCl_3$) δ 1.63 (br s, 1, NH, exchangeable with D_2O), 2.38 (s, 3, CH_3), 2.97 and 3.12 (two t, 4, CH_2NCH_2), 3.80 (s, 6, OCH_3), 4.16 (m, 4, OCH_2 and CH_2O), 5.09 (s, 2, CH_2Ar), 6.53−7.50 (m, 11, ArH). The oxalate salt was crystallized from EtOH; mp 155−156 °C. Anal. ($C_{26}H_{31}NO_5 \cdot H_2C_2O_4 \cdot 0.5H_2O$) C, H, N.

[2-(2,6-Dimethoxyphenoxy)ethyl]-{2-[2-(3-methylbenzyloxy)phenoxy]ethyl}amine (9). Eluting with $CHCl_3$/EtOH (9.9:0.1) gave **9** as the free base; (41% yield). ^1H NMR ($CDCl_3$) δ 1.78 (br s, 1, NH, exchangeable with D_2O), 2.32 (s, 3, CH_3), 2.99 and 3.12 (two t, 4, CH_2NCH_2), 3.82 (s, 6, OCH_3), 4.18 (m, 4, OCH_2 and CH_2O), 5.08 (s, 2, CH_2Ar), 6.53−7.28 (m, 11, ArH). The oxalate salt was crystallized from EtOH; mp 126−127 °C. Anal. ($C_{26}H_{31}NO_5 \cdot H_2C_2O_4 \cdot 0.25H_2O$) C, H, N.

[2-(2,6-Dimethoxyphenoxy)ethyl]-{2-[2-(4-methylbenzyloxy)phenoxy]ethyl}amine (10). Eluting with $CHCl_3$/EtOH (9.8:0.2) gave **10** as the free base; (42% yield). ^1H NMR ($CDCl_3$) δ 2.20 (br s, 1, NH, exchangeable with D_2O), 2.28 (s, 3, CH_3), 2.95 and 3.08 (two t, 4, CH_2NCH_2), 3.78 (s, 6, OCH_3), 4.12 (m, 4, OCH_2 and CH_2O), 5.05 (s, 2, CH_2Ar), 6.50−7.32 (m, 11, ArH). The oxalate salt was crystallized from EtOH; mp 145−146 °C. Anal. ($C_{26}H_{31}NO_5 \cdot H_2C_2O_4 \cdot 0.5H_2O$) C, H, N.

[2-(2,6-Dimethoxyphenoxy)ethyl]-{2-[2-(2-nitrobenzyloxy)phenoxy]ethyl}amine (11). Eluting with $CHCl_3$/EtOH (9.9:0.1) gave **11** as the free base; (49% yield). ^1H NMR ($CDCl_3$) δ 1.93 (br s, 1, NH, exchangeable with D_2O), 3.0 and 3.14 (two t, 4, CH_2NCH_2), 3.80 (s, 6, OCH_3), 4.19 (m, 4, OCH_2 and CH_2O), 5.52 (s, 2, CH_2Ar), 6.53−8.17 (m, 11, ArH). The oxalate salt was crystallized from MeOH; mp 171−172 °C. Anal. ($C_{25}H_{28}N_2O_7 \cdot H_2C_2O_4 \cdot 0.25H_2O$) C, H, N.

[2-(2,6-Dimethoxyphenoxy)ethyl]-{2-[2-(3-nitrobenzyloxy)phenoxy]ethyl}amine (12). Eluting with $CHCl_3$/EtOH (9.9:0.1) gave **12** as the free base; (45% yield). ^1H NMR ($CDCl_3$) δ 1.93 (br s, 1, NH, exchangeable with D_2O), 2.99 and 3.12 (two t, 4, CH_2NCH_2), 3.80 (s, 6, OCH_3), 4.19 (m, 4, OCH_2 and CH_2O), 5.21 (s, 2, CH_2Ar), 6.51−8.31 (m, 11, ArH). The oxalate salt was crystallized from EtOH; mp 137−138 °C. Anal. ($C_{25}H_{28}N_2O_7 \cdot H_2C_2O_4 \cdot 0.25H_2O$) C, H, N.

[2-(2,6-Dimethoxyphenoxy)ethyl]-{2-[2-(4-nitrobenzyloxy)phenoxy]ethyl}amine (13). Eluting with $CHCl_3$/EtOH (9.9:0.1) gave **13** as the free base; (24% yield). ^1H NMR ($CDCl_3$) δ 2.15 (br s, 1, NH, exchangeable with D_2O), 3.01 and 3.14 (two t, 4, CH_2NCH_2), 3.81 (s, 6, OCH_3), 4.20 (m, 4, OCH_2 and CH_2O), 5.20 (s, 2, CH_2Ar), 6.50−8.12 (m, 11, ArH). The oxalate salt was crystallized from EtOH; mp 167−168 °C. Anal. ($C_{25}H_{28}N_2O_7 \cdot H_2C_2O_4 \cdot 0.25H_2O$) C, H, N.

[2-(2-Benzyloxyphenoxy)ethyl]-[2-(2,6-dimethoxyphenoxy)ethyl]carbamic Acid Methyl Ester (23). Methyl chloroformate (0.45 mL; 5.82 mmol) was added dropwise to a stirred solution of *N*-[2-[2-(benzyloxy)phenoxy]ethyl]-*N*-[2-(2,6-dimethoxyphenoxy)ethyl]amine (**4**)[26] (1,95 g; 4.6 mmol) and Et_3N (0.65 mL; 4.6 mmol) in $CHCl_3$ (30 mL). Removal of solvent gave a residue, which was purified by column chromatography. Eluting with cyclohexane/AcOEt (8:2) gave an oil; 1.7 g (77% yield). ^1H NMR ($CDCl_3$) δ 3.62−4.0 (m, 13, OCH_3 and CH_2NCH_2), 4.02−4.30 (m, 4, OCH_2 and CH_2O), 5.09 (s, 2, CH_2Ar), 6.52−7.53 (m, 12, ArH).

[2-(2,6-Dimethoxyphenoxy)ethyl]-[2-(2-hydroxyphenoxy)ethyl]carbamic Acid Methyl Ester (24). A solution of **23** (1.1 g; 2.28 mmol) in EtOAc/AcOH (9:1; 5.7 mL) was hydrogenated over 10% Pd on charcoal (0.07 g) for 27 h at 50 psi of pressure. Following catalyst removal, the solution was diluted with Et_2O, and the extracts were washed with $NaHCO_3$ and ice. Removal of dried solvent gave an oil, which was purified by column chromatography. Eluting with cyclohexane/AcOEt (8:2) gave an oil; 0.58 g (65% yield). ^1H NMR ($CDCl_3$) δ 3.62−4.0 (m, 13, OCH_3 and CH_2NCH_2), 4.03−4.32 (m, 4, OCH_2 and CH_2O), 6.52−7.04 (m, 7, ArH).

[2-(2,6-Dimethoxyphenoxy)ethyl]-{2-[2-(2-methoxybenzyloxy)phenoxy]ethyl}carbamic Acid Methyl Ester (25a). A mixture of **24** (0.36 g; 0.92 mmol), 2-methoxybenzyl chloride (0.2 mL; 1.44 mmol), and K_2CO_3 (0.13 g; 0.94 mmol) in DMF (1.82 mL) was refluxed for 4 h at 125 °C. After cooling to 0 °C, a solution of 5% NaOH was added and the solution was extracted with Et_2O.The extracts were washed with 5% NaOH and H_2O. Removal of dried solvent gave a residue, which was purified by column chromatography. Eluting with petroleum ether/Et_2O (5:5) gave an oil; 0.43 g (91% yield). ^1H NMR ($CDCl_3$) δ 3.66−3.98 (m, 16, OCH_3 and CH_2NCH_2), 4.03−4.30 (m, 4, OCH_2 and CH_2O), 5.12 (s, 2, CH_2Ar), 6.52−7.53 (m, 11, ArH).

Similarly, compounds **25b**−**c** were obtained via the procedure described for **25a**.

[2-(2,6-Dimethoxyphenoxy)ethyl]-{2-[2-(3-methoxybenzyloxy)phenoxy]ethyl}carbamic Acid Methyl Ester (25b). 91% Yield. ^1H NMR ($CDCl_3$) δ 3.67−3.98 (m, 16, OCH_3 and CH_2NCH_2), 4.03−4.30 (m, 4, OCH_2 and CH_2O), 5.08 (s, 2, CH_2Ar), 6.52−7.32 (m, 11, ArH).

[2-(2,6-Dimethoxyphenoxy)ethyl]-{2-[2-(4-methoxybenzyloxy)phenoxy]ethyl}carbamic Acid Methyl Ester (25c). 73% Yield; mp 85−87 °C. ^1H NMR ($CDCl_3$) δ 3.67−3.94 (m, 16, OCH_3 and CH_2NCH_2), 4.01−4.25 (m, 4, OCH_2 and CH_2O), 5.02 (s, 2, CH_2Ar), 6.52−7.39 (m, 11, ArH).

[2-(2,6-Dimethoxyphenoxy)ethyl]-{2-[2-(4-ethoxybenzyloxy)phenoxy]ethyl}carbamic Acid Methyl Ester (26). A solution of DIAD (0.2 mL; 0.984 mmol) in dry THF (1.5 mL) was added dropwise to a solution of **24** (0.35; 0.894 mmol), 4-ethoxybenzyl alcohol (0.14 g; 0.894 mmol), and $(C_6H_5)_3P$ (0.235 g; 0.894 mmol) in dry THF (2 mL) with stirring under a stream of dry nitrogen. When the addition was completed, the reaction mixture was left for 2 h at room temperature. Removal of solvent gave a residue, which was purified by column chromatography. Eluting with cyclohexane/Et_2O (7:3) gave an oil; 0.25 g (52% yield). ^1H NMR ($CDCl_3$) δ 1.40 (t, 3, CH_2CH_3), 3.60−4.28 (m, 19, OCH_3, OCH_2CH_3, CH_2NCH_2, OCH_2, and CH_2O), 5.0 (s, 2, CH_2Ar), 6.52−7.38 (m, 11, ArH).

[2-(4-Isopropoxybenzyloxy)phenoxy]acetic Acid Methyl Ester (27). Compound **27** was obtained via the procedure described for **26** starting from (2-hydroxyphenoxy)acetic acid methyl ester (1.74; 9.56 mmol) and 4-isopropoxybenzyl alcohol (1.59 g; 9.56 mmol). Eluting solvent: cyclohexane/AcOEt (9.5:0.5); 41% yield; mp 75−76 °C. ^1H NMR ($CDCl_3$) δ 1.32 (d, 6, $CH(CH_3)_2$), 3.78 (s, 3, OCH_3), 4.55 (m, 1, $CH(CH_3)_2$), 4.70 (s, 2, OCH_2CO), 5.04 (s, 2, CH_2Ar), 6.80−7.40 (m, 8, ArH).

[2-(2,6-Dimethoxyphenoxy)ethyl]-{2-[2-(2-methoxybenzyloxy)phenoxy]ethyl}amine (14). A saturated solution of KOH (5 mL) was added to a solution of **25a** (0.43 g; 0.84 mmol) in MeOH (15 mL). The reaction mixture was refluxed for 48 h. Removal of solvent gave a residue, which was dissolved in H_2O and extracted with $CHCl_3$. Removal of dried solvent gave an oil as the free base; 0.15 g (39% yield). ^{1}H NMR ($CDCl_3$) δ 1.98 (br s, 1, NH, exchangeable with D_2O), 3.0 and 3.14 (two t, 4, CH_2NCH_2), 3.82 and 3.85 (two s, 9, OCH_3), 4.17 (m, 4, OCH_2 and CH_2O), 5.18 (s, 2, CH_2Ar), 6.52−7.52 (m, 11, ArH). The oxalate salt was crystallized from EtOH; mp 141−142 °C. Anal. ($C_{26}H_{31}NO_6{\cdot}H_2C_2O_4{\cdot}0.5H_2O$) C, H, N.

Similarly, compounds **15**−**17** were obtained via the procedure described for **14**.

[2-(2,6-Dimethoxyphenoxy)ethyl]-{2-[2-(3-methoxybenzyloxy)phenoxy]ethyl}amine (15). 48% Yield. ^{1}H NMR ($CDCl_3$) δ 1.84 (br s, 1, NH, exchangeable with D_2O), 3.0 and 3.12 (two t, 4, CH_2NCH_2), 3.79 and 3.81 (two s, 9, OCH_3), 4.18 (m, 4, OCH_2 and CH_2O), 5.11 (s, 2, CH_2Ar), 6.52−7.29 (m, 11, ArH). The oxalate salt was crystallized from EtOH; mp 117−118 °C. Anal. ($C_{26}H_{31}NO_6{\cdot}H_2C_2O_4$) C, H, N.

[2-(2,6-Dimethoxyphenoxy)ethyl]-{2-[2-(4-methoxybenzyloxy)phenoxy]ethyl}amine (16). 49% Yield. ^{1}H NMR ($CDCl_3$) δ 1.88 (br s, 1, NH, exchangeable with D_2O), 2.98 and 3.12 (two t, 4, CH_2NCH_2), 3.75 and 3.81 (two s, 9, OCH_3), 4.18 (m, 4, OCH_2 and CH_2O), 5.05 (s, 2, CH_2Ar), 6.53−7.40 (m, 11, ArH). The oxalate salt was crystallized from EtOH; mp 157−158 °C. Anal. ($C_{26}H_{31}NO_6{\cdot}H_2C_2O_4{\cdot}0.5H_2O$) C, H, N.

[2-(2,6-Dimethoxyphenoxy)ethyl]-{2-[2-(4-ethoxybenzyloxy)phenoxy]ethyl}amine (17). The free base was purified by column chromatography eluting with $CHCl_3$/EtOH (9.8:0.2); 50% yield. ^{1}H NMR ($CDCl_3$) δ 1.19 (t, 3, CH_2CH_3), 2.17 (br s, 1, NH, exchangeable with D_2O), 2.97 and 3.09 (two t, 4, CH_2NCH_2), 3.80 (s, 6, OCH_3), 3.97 (q, 2, CH_2CH_3), 4.15 (m, 4, OCH_2 and CH_2O), 5.02 (s, 2, CH_2Ar), 6.52−7.38 (m, 11, ArH). The oxalate salt was crystallized from EtOH/Et_2O; mp 136−137 °C. Anal. ($C_{27}H_{33}NO_6{\cdot}H_2C_2O_4{\cdot}H_2O$) C, H, N.

[2-(4-Isopropoxybenzyloxy)phenoxy]acetic Acid (28). A mixture of **27** (1.0 g; 3.03 mmol) and 2 N NaOH (25.0 mL) was stirred at 70 °C for 1.5 h. The mixture was extracted with $CHCl_3$, and the aqueous layer was acidified with concentrated HCl. Extraction with $CHCl_3$, followed by washing, drying, and evaporation of the extracts gave a solid (0.8 g; 83% yield), which was crystallized from cyclohexane; mp 55−56 °C. ^{1}H NMR ($CDCl_3$) δ 1.32 (d, 6, $CH(CH_3)_2$), 4.55 (m, 1, $CH(CH_3)_2$), 4.72 (s, 2, OCH_2CO), 5.17 (s, 2, CH_2Ar), 6.12 (br s, 1, COOH), 6.72−7.32 (m, 8, ArH).

***N*-[2-(2,6-Dimethoxyphenoxy)ethyl]-2-[2-(4-isopropoxybenzyloxy)phenoxy]acetamide (29).** Ethyl chloroformate (0.28 g; 2.53 mmol) was added dropwise to a stirred and cooled (0 °C) solution of **28** (0.8 g; 2.53 mmol) and Et_3N (0.26 g; 2.53 mmol) in $CHCl_3$ (50 mL), followed after 30 min by the addition of a solution of 2-(2,6-dimethoxyphenoxy)ethylamine[32] (0.5 g; 2.53 mmol) in $CHCl_3$ (10 mL). The resulting reaction mixture was stirred for 3 h at room temperature and then washed with 2 N HCl, 2 N NaOH, and finally water. Removal of dried solvent gave an oil, which was purified by column chromatography. Eluting with cyclohexane/AcOEt (6:4) gave an oil; 0.67 g (54% yield). ^{1}H NMR ($CDCl_3$) δ 1.32 (d, 6, $CH(CH_3)_2$), 3.57 (q, 2, NCH_2), 3.75 (s, 6, OCH_3) 4.08 (t, 2, CH_2O), 4.48 (m, 1, $CH(CH_3)_2$), 4.58 (s, 2, OCH_2CO), 5.04 (s, 2, CH_2Ar), 6.52−7.34 (m, 11, ArH), 7.92 (br t, 1, NH, exchangeable with D_2O).

[2-(2,6-Dimethoxyphenoxy)ethyl]-{2-[2-(4-isopropoxybenzyloxy)phenoxy]ethyl}amine (18). A solution of $BH_3{\cdot}Me_2S$ (0.3 mL) in dry THF (2 mL) was added dropwise at room temperature to a solution of **28** (0.67 g; 1.36 mmol) in dry THF (60 mL) with stirring under a stream of dry nitrogen with exclusion of moisture. When the addition was completed, the reaction mixture was heated at 70 °C for 6 h. After cooling to 0 °C, excess borane was destroyed by cautious dropwise addition of EtOH (1 mL). After standing overnight at room temperature, 2 N NaOH (3.3 mL) was added, and the resulting mixture was heated at 60 °C for 3 h. Removal of the solvent under reduced pressure gave a residue, which was dissolved in H_2O (10 mL) and ice. The aqueous solution was extracted with Et_2O. Removal of dried solvent gave a residue, which was purified by column chromatography. Eluting with cyclohexane/Et_2O/EtOH (5:5:1.5) afforded **18** as the free base: 0.33 g (62% yield). ^{1}H NMR ($CDCl_3$) δ 1.32 [d, 6, $CH(CH_3)_2$], 2.13 (br s, 1, NH, exchangeable with D_2O), 2.97 and 3.10 (two t, 4, CH_2-NCH_2), 3.80 (s, 6, OCH_3), 4.14 (m, 4, OCH_2 and CH_2O), 4.47 (m, 1, $CH(CH_3)_2$), 5.02 (s, 2, CH_2Ar), 6.52−7.37 (m, 11, ArH). The oxalate salt was crystallized from EtOH/Et_2O; mp 152−153 °C. Anal. ($C_{28}H_{35}NO_6{\cdot}H_2C_2O_4$) C, H, N.

Biology. Functional antagonism in isolated tissues and radioligand binding assays were performed according to the protocols reported in ref 41. Agonist efficacy, tested with [^{35}S]-GTPγS binding on cells transfected with human cloned 5-HT_{1A} serotoninergic receptors, was evaluated according to the protocol reported in ref 26.

Cell Culture. PC-3 ($p53^{-/-}$) human androgen-nonresponsive prostate cancer cells were purchased from the American Type Tissue Collection (Manassas, VA). Cells were cultured in Dulbecco's modified Eagle's medium (DMEM) (Gibco, BRL, Life Technology, Milan) supplemented with 10% fetal bovine serum, 2 mM L-glutamine (Euroclone, Devon) at 37 °C in a humidified incubator containing 5% CO_2.

Immunofluorescence and FACS Analysis. To determine the expression of α_{1B}- and α_{1D}-AR subtypes on the PC-3 line, 1×10^6 cells were fixed and permeabilized using CytoFix/CytoPerm Plus (BD Biosciences, Milano) before the addition of anti-α_{1B}-AR and anti- α_{1D}-AR polyclonal Abs (1:25 dilution). Normal goat serum and rabbit normal serum were used as negative controls. After 30 min at 4 °C, cells were washed twice and labeled with FITC-conjugated RAG and with FITC-conjugated GARB (1:20 dilution), respectively. In some experiments, PC-3 cells were exposed to the test agents, norepinephrine (NE) at the indicated concentration, alone or in combination, for 24 h, and stained as described above. The percentage of positive cells, determined over 10 000 events, was analyzed on a FACScan cytofluorimeter (Becton Dickinson, San José, CA). Fluorescent intensity is expressed in arbitrary units on a logarithmic scale.

Cell viability and apoptotic cell death were detected by flow cytometry using propidium iodide (PI) exclusion and Annexin V staining. PC-3 cells exposed to the test agents, NE at the indicated concentration, alone or in combination, for different times, were trypsinized and washed in PBS. Cells were then resuspended in PBS containing 40 μM of PI (Molecolar Probes, Leiden) for 30 min, and PI uptake was analyzed by cytofluorimetric and FACS analysis. Viability was defined as cells excluding PI and maintaining a high forward scatter.

Apoptotic cell death was evaluated by phosphatidylserine (PS) exposure on PC-3 cells by Annexin V staining.[44] Briefly, 1×10^6 PC-3 cells exposed to the test agents (50 μM) alone or in combination with NE (10 and 50 μM), for 24 h, were resuspended in 0.2 mL of binding buffer (10 mM Hepes/NaOH, pH 7.4, 150 mM NaCl, 5 mM KCl, 1 mM $MgCl_2$, 1.8 mM $CaCl_2$) in the presence of 5 μL of FITC-Annexin V (Bender MedSystem, Vienna) for 10 min at room temperature in the dark. The percentage of positive cells determined over 10 000 events was analyzed on a FACScan cytofluorimeter. Fluorescence intensity is expressed in arbitrary units on a logarithmic scale.

Confocal Laser Scanning Microscopy Analysis. 2×10^5/mL PC-3 cells, grown for 24 h at 37 °C and 5% CO_2 in poly-L-lysine-coated slides, were permeabilized using 2% of paraformaldehyde with 0.5% of Triton X-100 in PBS and fixed by 4% of paraformaldehyde in PBS. After three washes in PBS, cells were incubated with 3% of BSA and 0.1% of Tween-20 in PBS for 1 h at room temperature and then with a goat anti-α_{1B}-AR or a rabbit anti-α_{1D}-AR polyclonal Abs (1:50) at 4 °C overnight. Samples were finally washed with 0.3% of Triton X-100 in PBS three times, incubated with FITC-conjugated RAG Ab or with FITC-conjugated GARB Ab (1:100) for 1 h at 4 °C, mounted, and analyzed with a MRC600 confocal laser scanning microscope (BioRad, Hercules, CA) equipped with a Nikon (Diaphot-TMD) inverted microscope. Fluorochrome was excited with the 600 line of an argon-krypton laser and imaged using a 488

(FITC)-nm band-pass filter. Serial optical sections were taken at 1-μm intervals through the cells. Images were processed using Jacs Paint Shop Pro (Jacs Sotfware Inc).

Western Blot Analysis. Lysates obtained from PC-3 cells and human lymphocytes, used as positive control, were resuspended in 0.2 mL of RIPA (0.1% Nonidet-P40, 1 mM $CaCl_2$, 1 mM $MgCl_2$, 0.1% sodium azide, 1 mM PMSF, 0.03 mg/mL aprotinin, 1 mM $NaVO_4$). Samples were separated on 7.5% SDS-polyacrylamide gel, transferred onto Immobilon-P membranes (Millipore, Bedford, MA), and blotted with goat anti-α_{1B}-AR and a rabbit anti- α_{1D}-AR polyclonal Abs (1:400) followed by the incubation with HRP-conjugated RAG (1: 20000) and HPR-conjugated donkey anti-rabbit (1:10000) Abs, respectively. Immunoreactivity was detected using the Enhanced Chemiluminescence (ECL, Amersham) and the Chemidoc (Bio-Rad) apparatus.

RNA Isolation, Reverse Transcription and RT-PCR Analysis. Messenger RNA was extracted from PC-3 cells or human lymphocytes as positive control, using the Rnasy Mini Kit (Qiagen Sciences, MA). The mRNA samples resuspended in diethylpyrocarbonate (DEPC) water, and their concentration and purity were evaluated by A_{260} measurement. RNA samples (4 μg) were subjected to reverse transcription using the High Capacity cDNA Archive Kit protocol (RT buffer, dNTP mixture, Random Primers, MultiScribe RT, RNase inhibitor, Applied Biosystems, Monza). Two microliters of resulting cDNA products was used as template for Reverse Transcriptase (RT)-PCR.

RT-PCR was performed using a GeneAmp 5700 Sequence Detection system (Applied Biosystems, Monza). The reaction mixture contained the HotStarTaq Master Mix (Qiagen Sciences, Maryland) and primers.

α_1-AR subtypes primer sequences (forward and reverse) were as follows:

α_{1A}: 5′-AATGATACGGAACAGCATT-3′; 5′-GTGGCTGT-CAGTAGGTT-3′

α_{1B}: 5′-AGATGACTCCTGCCAG-3′; 5′-ACTGAGCAGCGC-CAAGAT-3′

α_{1D}: 5′-CTACGAATTGGCCGACT-3′; 5′-GGATGGGGCAGT-GTTTC-3′

Each PCR amplification consisted of heat activation for 15 min at 95 °C followed by 30 cycles of 94 °C for 30 s, 54 °C for 30 s and 72 °C for 30 s, by 30 cycles of 94 °C for 30 s, 52 °C for 30 s and 72 °C for 30 s and by 30 cycles of 94 °C for 30 s, 54 °C for 30 s and 72 °C for 30 s for α_{1A}-, α_{1B}- and α_{1D}-subtypes, respectively. PCR products were analyzed by electrophoresis on 1.5% ethidium bromide-stained agarose gel, visualized by UV transilluminator and acquired by a Chemi Doc (BioRad).

In Vitro Cytotoxicity Assay. In vitro cytotoxicity was evaluated by SRB assay.[43] Cells were maintained as stocks in DMEM (Gibco) supplemented with 10% fetal bovine serum (Gibco), 2 mM L-glutamine (Gibco). Cell cultures were passaged twice weekly using trypsin-EDTA to detach the cells from their culture flasks. The rapidly growing cells were harvested, counted, and incubated under the appropriate concentrations (7×10^5 cells/well) in 96-well microtiter plates. After incubation for 24 h, target and test agents dissolved in culture medium were applied to the culture wells in quadruplicate and incubated for 48 h at 37 °C in a 5% CO_2 atmosphere and 95% relative humidity. At the same time, a plate was tested to evaluate the cell population before addition of the test agents addition (Tz). In some experiments, an SRB assay was performed using the test agents in combination with 0.1 μM of the 5-HT_{1A} antagonist, (*S*)-WAY 100135. Culture, fixed with cold trichloroacetic acid (TCA), was stained by 0.4% SRB dissolved in 1% acetic acid. Bound stains were subsequently solubilized with 10 mM Trizma, and the absorbance was read on the microplate reader Dynatech Model MR 700 at a wavelength of 520 nm. The cytotoxic activity was evaluated by measuring the drug concentration resulting in a 50% reduction in the net protein increase (as measured by SRB staining) in control cells during the drug incubation (GI_{50}), that resulting in total growth inhibition (TGI), and that resulting in a 50% reduction in the measured protein at the end of the drug treatment, as compared to that at the beginning (LC_{50}). The percentage of growth inhibition was calculated as $[(Ti - Tz)/(C - Tz)] \times 100$ for concentrations for which $Ti \geq Tz$ and $[(Ti - Tz)/Tz] \times 100$ for those for which $Ti < Tz$, where Tz = absorbance time zero, C = absorbance in the presence of vehicle, and Ti = absorbance in the presence of drug at different concentrations. GI_{50}, TGI and LC_{50} were obtained by interpolating % of growth versus Log(M) in a graph. Each quoted value represents the mean of quadruplicate determinations.

Proliferation Assay. A total of 7×10^4 PC-3 cells, dispersed for 24 h into tissue cultured-treated plastic 96-well flat-bottomed microtiter plates at 37 °C, 5% CO_2 humidified air atmosphere, were incubated with different doses of NE (0, 0.1, 1, 10, and 50 μM) alone or in combination with compound **4** and doxazosin (1 μM) or compound **7** (0.5 μM), for 16 h in a total volume of 200 μL of culture medium. During the last 4 h, all samples received the addition of the pyrimidine analogue BrdU, that, after incorporation into the DNA of proliferating cells, was detected by immunoassay using a Cell Proliferation ELISA BrdU (colorimetric) kit (Boehringer Mannheim, Roche).

Statistical Analysis. Statistical significance was determined by using analysis of variance (ANOVA) followed by post hoc Newman-Keuls multiple comparison at $P < 0.01$ and by Student's *t*-test at $P < 0.01$.

Acknowledgment. We thank the MIUR (Rome) and the University of Camerino for financial support.

Supporting Information Available: Elemental analysis. This material is available free of charge via the Internet at http://pubs.acs.org.

References

(1) For part 7, see ref 41.
(2) (a) Calzada, B. C.; De Artinano A. A. α-Adrenoceptors Subtypes. *Pharmacol. Res.* **2001**, *44*, 195−208. (b) Piascik, M. T.; Perez, D. M. α_1-Adrenergic Receptors: New Insights and Directions. *J. Pharmacol. Exp. Ther.* **2001**, *298*, 403−410.
(3) Daniels, D. V.; Gever, J. R.; Jasper, J. R.; Kava, M. S.; Lesnick, J. D.; Meloy, T. D.; Stepan, G.; Williams, T. J.; Clarke, D. E.; Chang, D. J.; Ford, A. P. Human Cloned α_{1A}-Adrenoceptor Isoforms Display α_{1L}-Adrenoceptor Pharmacology in Functional Studies. *Eur. J. Pharmacol.* **1999**, *370*, 337−343.
(4) Price, D. T.; Schwinn, D. A.; Lomasney, J. W.; Allen, L. F.; Caron, M. G.; Lefkowitz, R. J. Identification, Quantification, and Localization of mRNA for Three Distinct α_1-Adrenergic Receptor Subtypes in Human Prostate. *J. Urol.* **1993**, *150*, 546−551.
(5) Walden, P. D.; Gerardi, C.; Lepor, H. Localization and Expression of the α_{1A}-, α_{1B}- and α_{1D}-Adrenoceptors in Hyperplastic and Non-Hyperplastic Human Prostate. *J. Urol.* **1999**, *161*, 635−640.
(6) (a) Tseng-Crank, J.; Kost, T.; Goetz, A.; Hazum, S.; Roberson, K. M.; Haizlip, J.; Godinot, N.; Robertson, C. N.; Saussy, D. The α_{1C}-Adrenoceptor in Human Prostate: Cloning, Functional Expression, and Localization to Specific Prostate Cell Types. *Br. J. Pharmacol.* **1995**, *115*, 1475−1485. (b) Moriyama, N.; Kurimoto, S.; Horie, S.; Nasu, K.; Tanaka, T.; Yano, K.; Hirano, H.; Tsujimoto, G.; Kawabe, K. Detection of α_1-Adrenoceptor Subtypes in Human Hypertrophied Prostate by in Situ Hybridization. *Histochem. J.* **1996**, *28*, 283−288.
(7) Thebault, S.; Roudbaraki, M.; Sydorenko, V.; Shuba, Y.; Lemonnier, L.; Slomianny, C.; Dewailly, E.; Bonnal, J. L.; Mauroy, B.; Skryma, R.; Prevarskaya, N. α_1-Adrenergic Receptors Activate Ca(2+)-Permeable Cationic Channels in Prostate Cancer Epithelial Cells. *J. Clin. Invest.* **2003**, *111*, 1691−1701.
(8) Kyprianou, N.; Benning, C. M. Suppression of Human Prostate Cancer Cell Growth by α_1-Adrenoceptor Antagonists Doxazosin and Terazosin via Induction of Apoptosis. *Cancer Res.* **2000**, *60*, 4550−4555.
(9) (a) Caine, M. α-Adrenergic Blockers for the Treatment of Benign Prostatic Hyperplasia. *Urol. Clin. North Am.* **1990**, *17*, 641−649. (b) Thorpe, A.; Neal, D. Benign Prostatic Hyperplasia. *Lancet* **2003**, *361*, 1359−1367.
(10) Benning, C. M.; Kyprianou, N. Quinazoline-Derived α_1-Adrenoceptor Antagonists Induce Prostate Cancer Apoptosis via an α_1-Adrenoceptor-Independent Action. *Cancer Res.* **2002**, *62*, 597−602.
(11) Yang, G.; Timme, T. L.; Park, S. H.; Wu, X.; Wyllie, M. G.; Thompson, T. C. Transforming Growth Factor beta 1 Transduced Mouse Prostate Reconstitutions: II. Induction of Apoptosis by Doxazosin. *Prostate* **1997**, *33*, 157−163.

(12) Partin, J. V.; Anglin, I. E.; Kyprianou, N. Quinazoline-Based α_1-Adrenoceptor Antagonists Induce Prostate Cancer Cell Apoptosis via TGF-beta Signalling and I kappa B alpha Induction. *Br. J. Cancer* **2003**, *88*, 1615−1621.
(13) Dizeyi, N.; Bjartell, A.; Nilsson, E.; Hansson, J.; Gadaleanu, V.; Cross, N.; Abrahamsson, P. A. Expression of Serotonin Receptors and Role of Serotonin in Human Prostate Cancer Tissue and Cell Lines. *Prostate* **2004**, *59*, 328−336.
(14) Keledjian, K.; Kyprianou, N. Anoikis Induction by Quinazoline Based α_1-Adrenoceptor Antagonists in Prostate Cancer Cells: Antagonistic Effect of bcl-2. *J. Urol.* **2003**, *169*, 1150−1156.
(15) Xu, K.; Wang, X.; Ling, P. M.; Tsao, S. W.; Wong, Y. C. The α_1-Adrenoceptor Antagonist Terazosin Induces Prostate Cancer Cell Death through a p53 and Rb Independent Pathway. *Oncol. Rep*. **2003**, *10*, 1555−1560.
(16) Zeng, L.; Rowland, R. G.; Lele, S. M.; Kyprianou, N. Apoptosis Incidence and Protein Expression of p53, TGF-beta Receptor II, p27Kip1, and Smad4 in Benign, Premalignant, and Malignant Human Prostate. *Hum. Pathol*. **2004**, *35*, 290−297.
(17) Noveral, J. P.; Grunstein, M. M. Adrenergic Receptor-Mediated Regulation of Cultured Rabbit Airway Smooth Muscle Cell Proliferation. *Am. J. Physiol.* **1994**, *267*, 291−299.
(18) Mimura, Y.; Kobayashi, S.; Notoya, K.; Okabe, M.; Kimura, I.; Horikoshi, I.; Kimura, M. Activation by α_1-Adrenergic Agonists of the Progression Phase in the Proliferation of Primary Cultures of Smooth Muscle Cells in Mouse and Rat Aorta. *Biol. Pharm. Bull.* **1995**, *18*, 1373−1376.
(19) Gao, B. B.; Lei, B. L.; Zhang, Y. Y.; Han, Q. D. Cell Proliferation and Ca(2+)-Calmodulin Dependent Protein Kinase Activation Mediated by α_{1A}-and α_{1B}-Adrenergic Receptors in HEK293 Cells. *Acta Pharmacol. Sin.* **2000**, *21*, 55−59.
(20) McVary, K. T.; McKenna, K.E.; Lee, C. Prostate Innervation. *Prostate Suppl.* **1998**, *8*, 2−13.
(21) Xin, X.; Yang, N.; Eckhart, A. D.; Faber, J. E. α_{1D}-Adrenergic Receptors and Mitogen-Activated Protein Kinase Mediate Increased Protein Synthesis by Arterial Smooth Muscle. *Mol. Pharmacol*. **1997**, *51*, 764−775.
(22) Kanagawa, K.; Sugimura, K.; Kuratsukuri, K.; Ikemoto, S.; Kishimoto, T.; Nakatani, T. Norepinephrine Activates P44 and P42 MAPK in Human Prostate Stromal and Smooth Muscle Cells but not in Epithelial Cells. *Prostate* **2003**, *56*, 313−318.
(23) Mottram, D. R.; Kapur, H. The α-Adrenoceptor Blocking Effects of a New Benzodioxane. *J. Pharm. Pharmacol.* **1975**, *27*, 295−296.
(24) Quaglia, W.; Pigini, M.; Giannella M.; Melchiorre, C. 3-Phenyl Analogues of 2-([(2-(2,6-Dimethoxyphenoxy)ethyl]amino]-methyl)-1,4-benzodioxan (WB 4101) as Highly Selective α_1-Adrenoreceptor Antagonists. *J. Med. Chem.* **1990**, *33*, 2946−2948.
(25) Quaglia, W.; Pigini, M.; Tayebati, S. K.; Piergentili, A.; Giannella, M.; Marucci, G.; Melchiorre, C. Structure−Activity Relationships in 1,4-Benzodioxan-Related Compounds. 4. Effect of Aryl and Alkyl Substituents at Position 3 on α-Adrenoreceptor Blocking Activity. *J. Med. Chem.* **1993**, *36*, 1520−1528.
(26) Quaglia, W.; Pigini, M.; Piergentili, A.; Giannella, M.; Marucci, G.; Poggesi, E.; Leonardi, A.; Melchiorre, C. Structure−Activity Relationships in 1,4-Benzodioxan-Related Compounds. 6. Role of the Dioxane Unit on Selectivity for α_1-Adrenoreceptor Subtypes. *J. Med. Chem.* **1999**, *42*, 2961−2968.
(27) Zhao, M. M.; Hwa, J.; Perez, D. M. Identification of Critical Extracellular Loop Residues Involved in α_1-Adrenergic Receptor Subtype-Selective Antagonist Binding. *Mol. Pharmacol.* **1996**, *50*, 1118−1126.
(28) Hamaguchi, N.; True, T. A.; Saussy, D. L., Jr.; Jeffs, P. W. Phenylalanine in the Second Membrane-Spanning Domain of α_{1A}-Adrenergic Receptor Determines Subtype Selectivity of Dihydropyridine Antagonists. *Biochemistry* **1996**, *35*, 14312−14317.
(29) Topliss J. G. Utilization of Operational Schemes for Analogue Synthesis in Drug Design. *J. Med. Chem.* **1972**, *15*, 1006−1011.
(30) Topliss J. G. A Manual Method for Applying the Hansch Approach to Drug Design. *J. Med. Chem.* **1977**, *20*, 463−469.
(31) Keledjian, K.; Borkowski, A.; Kim, G.; Isaacs, J. T.; Jacobs S. C.; Kyprianou, N. Reduction of Human Prostate Tumor Vascularity by the α_1-Adrenoceptor Antagonist Terazosin. *Prostate* **2001**, *48*, 71−78.
(32) Woolley, D. W. Probable Evolutionary Relations of Serotonin and Indole-Acetic Acid, and Some Practical Consequences Therefrom. *Nature (London)* **1957**, *180*, 630−633.
(33) Hancock, A. A.; Buckner, S. A.; Brune, M. E.; Katwala, S.; Milicic, I.; Ireland, L. M.; Morse, P. A.; Knepper, S. M.; Meyer, M. D.; Chapple, C. R.; Chess-Williams, R.; Noble, A. J.; Williams, M.; Kerwin, J. F., Jr. Pharmacological Characterization of A-131701, a Novel α_1-Adrenoceptor Antagonist Selective for α_{1A}- and α_{1D}-Compared to α_{1B}-Adrenoceptors. *Drug Dev. Res.* **1998**, *44*, 140−162.
(34) Testa, R.; Taddei, C.; Poggesi, E.; Destefani, C.; Cotecchia, S.; Hieble, J. P.; Sulpizio, A. C.; Naselsky, D.; Bergsma, D.; Ellis, S.; Swift, A.; Ganguly, S.; Ruffolo, R. R.; Leonardi, A. Rec 15/2739 (SB 216469): a Novel Prostate Selective α_1-Adrenoceptor Antagonist. *Pharmacol Commun.* **1995**, *6*, 79−86.
(35) (a) Fargin, A.; Raymond, J. R.; Lohse, M. J.; Kobilka, B. K.; Caron, M. G.; Lefkowitz, R. J. The Genomic Clone G-21 Which Resembles a β-Adrenergic Receptor Sequence Encodes the 5-HT_{1A} Receptor. *Nature* **1988**, *335*, 358−360. (b) Fargin, A.; Raymond, J. R.; Regan, J. W.; Cotecchia, S.; Lefkowitz, R. J.; Caron, M. G. Effector Coupling Mechanisms of the Cloned 5-HT_{1A} Receptor. *J. Biol. Chem.* **1989**, *284*, 14848−14852.
(36) Eltze, M.; Boer, R.; Sanders, K. H.; Kolossa, N. Vasodilatation Elicited by 5-HT_{1A} Receptor Agonists in Constant-Pressure-Perfused Rat Kidney Is Mediated by Blockade of α_{1A}-Adrenoreceptors. *Eur. J. Pharmacol*. **1991**, *202*, 33−44.
(37) Ko, F. N.; Guh, J. H.; Yu, S. M.; Hou, Y. S.; Wu, Y. C.; Teng, C. M. (−)-Discretamine, a Selective α_{1D}-Adrenoreceptor Antagonist, Isolated from *Fissistigma glaucescens*. *Br. J. Pharmacol.* **1994**, *112*, 1174−1180.
(38) Buckner, S. A.; Oheim, K. W.; Morse, P. A.; Knepper, S. M.; Hancock, A. A. α_1-Adrenoceptor-Induced Contractility in Rat Aorta Is Mediated by the α_{1D} Subtype. *Eur. J. Pharmacol.* **1996**, *297*, 241−248.
(39) van Rossum, J. M. Cumulative Dose−Response Curves. II. Technique for the Making of Dose−Response Curves in Isolated Organs and the Evaluation of Drug Parameters. *Arch. Int. Pharmacodyn. Ther.* **1963**, *143*, 299−330.
(40) Stanton, J. A.; Beer, M. S. Characterization of a Cloned Human 5-HT_{1A} Receptor Cell Line Using [^{35}S]GTPγS Binding. *Eur. J. Pharmacol.* **1997**, *320*, 267−275.
(41) Quaglia, W.; Pigini, M.; Piergentili, A.; Giannella, M.; Gentili, F.; Marucci, G.; Carrieri, A.; Carotti, A.; Poggesi E.; Leonardi, A.; Melchiorre C. Structure−Activity Relationships in 1,4-Benzodioxan-Related Compounds. 7. Selectivity of 4-Phenylchroman Analogues for α_1-Adrenoreceptor Subtypes. *J. Med. Chem.* **2002**, *45*, 1633−1643.
(42) Cal, C.; Uslu, R.; Gunaydin, G.; Ozyurt, C.; Omay, S. B. Doxazosin: a New Cytotoxic Agent for Prostate Cancer? *BJU Int.* **2000**, *85*, 672−675.
(43) Grever, M. R.; Shepartz, S. A.; Chabner, B. A. The National Cancer Institute: Cancer Drug Discovery and Development Program. *Semin. Oncol.* **1992**, *19*, 622−638.
(44) Vermes, I.; Haanen, C.; Steffens-Nakken, H.; Reutelingsperger, C. A Novel Assay for Apoptosis. Flow Cytometric Detection of Phosphatidylserine Expression on Early Apoptotic Cells Using Fluorescein Labelled Annexin V. *J. Immunol. Methods* **1995**, *184*, 39−51.
(45) Lindquist, J. M.; Rehnmark, S. Ambient Temperature Regulation of Apoptosis in Brown Adipose Tissue. Erk1/2 Promotes Norepinephrine-Dependent Cell Survival. *J. Biol. Chem*. **1998**, *273*, 30147−30156.
(46) Noh, J. S.; Kim, E. Y.; Kang, J. S.; Kim, H. R.; Oh, Y. J.; Gwag, B. J. Neurotoxic and Neuroprotective Actions of Catecholamines in Cortical Neurons. *Exp. Neurol.* **1999**, *159*, 217−224.
(47) Popovik, E.; Haynes, L. W. Survival and Mitogenesis of Neuroepithelial Cells Are Influenced by Noradrenergic but not Cholinergic Innervation in Culture Embryonic Rat Neopallium. *Brain Res.* **2000**, *853*, 227−235.
(48) Garcia-Sainz, J. A.; Villalobos-Molina, R. The Elusive α_{1D}-Adrenoceptor: Molecular and Cellular Characteristics and Integrative Roles. *Eur. J. Pharmacol*. **2004**, *500*, 113−120.
(49) Garcia-Sainz, J. A.; Rodriguez-Perez, C. E.; Romero-Avila, M. T. Human α_{1D}-Adrenoceptor Phosphorylation and Desensitization. *Biochem. Pharmacol*. **2004**, *67*, 1853−1858.
(50) Hague, C.; Uberti, M. A.; Chen, Z.; Hall, R.A.; Minneman, K. P. Cell Surface Expression of α_{1D}-Adrenergic Receptors Is Controlled by Heterodimerization with α_{1B}-Adrenergic Receptors. *J. Biol. Chem*. **2004**, *279*, 15541−15549.
(51) Cheng, Y.; Prusoff, W. H. Relationship Between the Inhibition Constant (K_i) and the Concentration of Inhibitor Which Causes 50% Inhibition (I_{50}) of an Enzymatic Reaction. *Biochem. Pharmacol.* **1973**, *22*, 3099−3108.

JM0580398